JOURNAL OF GUIDANCE, CONTROL, AND DYNAMICS
Vol. 36, No. 2, March–April 2013

Aircraft Endurance Maximization at Medium Mach Numbers by Extremum Seeking

James P. Krieger* and Miroslav Krstic†
University of California, San Diego, La Jolla, California 92093-0411

DOI: 10.2514/1.58364

Aircraft endurance is maximized by optimizing the lift to drag ratio over a two-dimensional space spanned by the angle of attack and the Mach number, constrained to a one-dimensional curve on which the lift equals the weight of the aircraft. The gradient estimator used in the optimization is excited by atmospheric turbulence in the vertical and longitudinal directions. This new form of extremum seeking requires a reformulation of the standard gradient estimator used in extremum seeking to provide gradient estimates that are independent of the amplitude of the dither signal. A new gradient estimator based on an estimation error approach is presented to this end. Through stochastic averaging analysis, the estimator is shown to stabilize the aircraft to the optimal endurance speed, with a bias that is proportional to the square of the turbulence amplitude and thus is small when the turbulence is light. The controller is tested in a high-fidelity six-degree-of-freedom simulation provided by local industry. Simulation results show the maximization of aircraft endurance and even a slight improvement compared to flight at the nominal loiter speed of the aircraft being simulated.

Nomenclature

A	=	aspect ratio
a	=	speed of sound
a_x, a_z	=	components of acceleration in the x- or z-body-axis directions
a_1, a_2	=	stochastic disturbance postsaturation scaling factors
C_D	=	coefficient of drag
C_{D0}	=	zero-lift drag coefficient
C_L	=	coefficient of lift
C_2, C_4	=	averaging constants
D	=	drag
e	=	Oswald efficiency number
f	=	lift to drag ratio
$\hat{f}$	=	estimator's prediction of f
g	=	acceleration due to gravity
g_x, g_z	=	components of g in the x- or z-body-axis directions
J	=	Jacobian of a system
k_{ES}	=	extremum-seeking gain
k_1, k_2, k_3	=	estimator gains
L	=	lift
L_u, L_v, L_w	=	characteristic lengths of the turbulence field (longitudinal, lateral, vertical)
M	=	Mach number
m	=	mass of the aircraft
$n_0, n_1, n_2, \ldots$	=	coefficients of the Taylor expansion of v
q_1, q_2	=	stochastic disturbance presaturation scaling factors
S	=	reference area
s	=	Laplace variable
s_1	=	estimator state (approximates f)
s_2	=	estimator state (approximates f_U)
s_3	=	estimator state (approximates f_V)
T	=	thrust
t	=	time
U	=	equivalent steady-state airspeed
U_0	=	nominal airspeed for the turbulence model
V	=	airspeed
v	=	zero-wind airspeed (roughly ground speed)
V_{cmd}	=	commanded airspeed
V_*	=	optimal endurance speed
v_{eq}	=	equilibrium airspeed of the average system
W_1, W_2	=	instances of standard Brownian motion
α	=	angle of attack
ϵ_1, ϵ_2	=	turbulence time constants
η_1, η_2	=	vertical and longitudinal wind speeds, presaturation
λ	=	thrust angle
$\mu(\mathrm{d}\eta)$	=	invariant distribution of η
ρ	=	air density
σ_2, σ_3	=	control law design parameters
σ_u, σ_v, σ_w	=	root mean square turbulence intensity (longitudinal, lateral, and vertical components)
τ	=	airspeed control time constant
Φ_{u_g}, Φ_{v_g}, Φ_{w_g}	=	turbulence spectra (longitudinal, lateral, vertical)
Ω	=	spatial frequency
ω	=	temporal frequency

Subscripts

eq	=	evaluated at the equilibrium point (i.e. let U and V both equal v_{eq})
U	=	partial derivative with respect to U
V	=	partial derivative with respect to V
v	=	evaluated at an arbitrary airspeed (i.e. let U and V both equal v)
0	=	evaluated at the center of the Taylor expansion
$*$	=	evaluated at the optimal endurance speed (i.e. let U and V both equal V_*)

Received 22 March 2012; revision received 8 August 2012; accepted for publication 18 August 2012; published online 12 February 2013.

*Graduate, Department of Mechanical and Aerospace Engineering, 9500 Gilman Dr. # 0411; jkrieger@ucsd.edu.

†Professor, Department of Mechanical and Aerospace Engineering, 9500 Gilman Dr. # 0411; krstic@ucsd.edu.

Introduction

THIS paper is a continuation of the research effort begun in [1], in which the authors present a control algorithm for finding the speed for maximum endurance for a jet aircraft. Flight at the speed for maximum endurance produces the minimum fuel burn rate, allowing

the longest duration of flight. The control algorithm in [1] is a novel form of extremum-seeking control in which atmospheric turbulence is used as the dither signal. The present work expands the basic principle developed in [1] by introducing a new algorithm capable of functioning at speeds in which compressibility becomes a factor. The algorithm is tested using a high-fidelity flight-test validated aircraft simulation program.

Extremum seeking traditionally involves adding a small perturbation, called a dither signal, to the input to a system. The resulting change in the output from the system is then used to determine whether the input should be increased or decreased to drive the output towards its minimum (or maximum) possible value. The dither signal is traditionally chosen to be sinusoidal [2–6] but can also be chosen to be nonsinusoidal [7] or stochastic [8,9]. Recently, the need for adding a dither signal has been removed by using naturally occurring disturbances in their stead [10]. The general applicability of extremum seeking has encouraged its use for a large variety of applications, including axial flow compressors [11], lean premixed combustion [12–14], flow control [15,16], wind turbine energy capture [17], the minimization of drag in formation flight [18], and many other applications in which the process dynamics may not be well known [19–30].

The authors' previous work [1] introduces a novel variant of extremum seeking intended to optimize the speed of a jet aircraft for optimal endurance. The primary assumptions in [1], which are here removed, are the following:

Assumption 1: The pitch and altitude dynamics of the aircraft can be considered quasi steady.

Assumption 2: The vertical component of turbulence is negligible.

Assumption 3: The effect of compressibility is negligible.

The first assumption is removed by optimizing the lift to drag ratio over the (two-dimensional) Mach vs angle-of-attack plane, rather than optimizing the drag itself over the airspeed in one dimension only. The pitch and altitude dynamics can significantly affect the drag of an aircraft, and so an algorithm based on an estimate of the rate of change of the drag with respect to airspeed can only function on a timescale much slower than the aircraft dynamics. Conversely, the lift to drag ratio is very nearly a static map in the Mach vs angle-of-attack plane; an approximation of such a map is not significantly restricted by the timescale of the aircraft dynamics.

The second assumption can (and actually must) be removed because the optimization is performed over a two-dimensional map, and as such, two independent dither signals are required: the longitudinal and vertical components of the atmospheric turbulence. (As explained in [31], a standard assumption in turbulence modeling is that the components of turbulence are independent stochastic processes.)

The third assumption is addressed explicitly by letting the lift to drag ratio be a function of the Mach number, as already mentioned.

And so, the removal of the preceding assumptions is achieved by optimizing the lift to drag ratio over a two-dimensional space. Atmospheric turbulence, having independent longitudinal and vertical components, provides excitation over the two-dimensional space. This is used to produce an estimate of the local two-dimensional gradient, that is, to produce an estimate of the slope of the lift to drag ratio with respect to the Mach number and an estimate of the slope with respect to the angle of attack. In a typical multidimensional application, extremum seeking is then used to find the maximizing point in the two-dimensional space; however, the aircraft cannot move freely in two dimensions. Rather, to achieve level flight it must fly at a combination of Mach number and angle of attack that produces a lift equal to the weight of the aircraft: a one-dimensional curve in a two-dimensional space.

Optimization over this curve is achieved by calculating the inner product of the gradient estimate with a vector locally tangent to the curve. This inner product gives the slope of the lift to drag ratio along the curve, which indicates whether a faster or slower airspeed would improve the lift to drag ratio. Here, the standard extremum-seeking algorithm fails: it produces an estimate of the gradient vector that points in the wrong direction. (An explanation now follows.) The standard multidimensional gradient estimator operates by demodulating the output with the two independent dither signals. This produces an estimate of the gradient in which each component is scaled by the variance of its respective dither signal. (This is acceptable because, at the maximum of a two-dimensional map, the gradient is zero, and the zero vector is zero no matter how its components are scaled.) At the optimal point along the curve of constant lift, the gradient should be perpendicular to the curve, but it should not, in general, be zero. If the components of the gradient are unequally scaled, the direction of the gradient will be incorrect, and the calculated inner product will be incorrect. This causes the optimization to fail. Of course, this can be corrected if the relative amplitudes of the dither signals are known, but in an application that uses atmospheric turbulence to provide the dither signals, the relative amplitude of the dither signals is not known.

This difficulty motivates the development of a new form of the gradient estimator, one based on estimation error rather than simple demodulation. A three-state gradient estimator is developed that creates an estimate of the lift to drag ratio based on the measured Mach number and angle of attack. The states represent 1) the lift to drag ratio at the current average Mach number and angle of attack, 2) the slope with the angle of attack, and 3) the slope with the Mach number. The difference between the estimated and the measured lift to drag ratios is used as feedback for the gradient estimator. As the states converge, the estimation error approaches zero. The critical feature of this design is that the equilibrium value of the gradient estimate does not depend on the amplitudes of the dither signals. The gradient estimate can be used to accurately determine the slope along the curve of constant lift. With this estimate of the slope, the optimal endurance speed can be accurately found.

The paper begins with an overview of the relevant aerodynamics. An extremum-seeking algorithm is then developed that finds the optimal endurance speed. (The new form of the gradient estimator is developed at this point.) Convergence to the optimal airspeed is then shown through analysis, and the algorithm is tested in simulation.

Aerodynamics

This section presents the background aerodynamics information relevant to the following control development. Additional background can be found in [32].

Optimal Endurance

Endurance is the length of time an aircraft can remain airborne. For jet aircraft, the endurance in level flight may be optimized by flying at an airspeed that minimizes drag or, equivalently, that maximizes the lift to drag ratio. The lift to drag ratio is a function of several variables, the most important, perhaps, being the angle of attack. In compressible flows, the Mach number also has a significant effect. As a function of the angle of attack and Mach number, the optimal lift to drag ratio is found at a point in a two-dimensional space; however, to maintain level flight, the aircraft must fly at a combination of Mach number and angle of attack that produces a lift equal to the weight of the aircraft. That is, in level flight, an aircraft is constrained to a curve of constant lift in a two-dimensional (Mach number, angle of attack) space. The optimal endurance speed corresponds to the point on this curve that produces the highest lift to drag ratio.

The optimal endurance speed generally varies with aircraft weight and altitude. However, under certain common assumptions, it can be shown that optimal endurance occurs at the same coefficient of lift. Assume that the coefficient of lift increases with the Mach number as $1/\sqrt{1-M^2}$ according to the Prandtl–Glauert rule. Assume a quadratic drag polar that does not change with the Mach number. (Accounting for compressibility effects in this manner is valid for Mach numbers less than about 0.75 [33].) These two assumptions are expressed as

$$C_L = \frac{C_L|_{M=0}}{\sqrt{1-M^2}} \tag{1}$$

$$C_D = C_{D0} + \frac{(C_L|_{M=0})^2}{\pi Ae} \tag{2}$$

The lift to drag ratio is then

$$f = \frac{L}{D} = \frac{C_L(1/2)\rho V^2 S}{C_D(1/2)\rho V^2 S} = \frac{C_L}{C_D} = \frac{C_L}{C_{D0} + [(C_L|_{M=0})^2/\pi Ae]}$$
$$= \frac{C_L}{C_{D0} + (C_L^2/\pi Ae)(1 - M^2)} \tag{3}$$

The Mach number can be expressed in terms of lift and C_L as

$$M = \frac{V}{a} = \frac{1}{a}\sqrt{\frac{L}{C_L(1/2)\rho S}} = \sqrt{\frac{L}{C_L(1/2)\rho a^2 S}} \tag{4}$$

and so, the lift to drag ratio can be written as a function of lift and C_L,

$$f(C_L, L) = \frac{C_L}{C_{D0} + (C_L^2/\pi Ae)\{1 - [L/C_L(1/2)\rho a^2 S]\}}$$
$$= \frac{C_L}{C_{D0} - [C_L L/\pi Ae(1/2)\rho a^2 S] + (C_L^2/\pi Ae)} \tag{5}$$

The lift to drag ratio at any given value of lift is maximized when the partial derivative with respect to C_L is zero. The partial derivative is

$$\frac{\partial f(C_L, L)}{\partial C_L} = \frac{C_{D0} - (C_L^2/\pi Ae)}{\{C_{D0} - [C_L L/\pi Ae(1/2)\rho a^2 S] + (C_L^2/\pi Ae)\}^2} \tag{6}$$

Setting this equal to zero and solving for the coefficient of lift gives

$$C_L = \sqrt{C_{D0}\pi Ae} \tag{7}$$

This optimal C_L is a constant depending only on the parameters of the quadratic drag polar. It does not vary with density or lift. Under the assumption of a quadratic drag polar and the Prandtl–Glauert rule, the optimal airspeed for a certain flight condition can be related to the optimal airspeed at another altitude or aircraft weight by equating the coefficients of lift.

Measurement of Lift and Drag

Although lift and drag are not directly measurable, they can be computed based on other quantities that may be more readily available. They can be calculated based on longitudinal and vertical body-axis accelerometer measurements [$(a_x - g_x)$ and $(a_z - g_z)$, respectively] and estimates of the aircraft mass m, engine thrust T, and thrust angle λ. Using a free-body diagram like the one shown in Fig. 1, the lift can be calculated from the measured and estimated variables as

$$L = \sin\alpha[-T\cos\lambda + m(a_x - g_x)]$$
$$+ \cos\alpha[-T\sin\lambda + m(a_z - g_z)] \tag{8}$$

and, the drag can be calculated as

$$D = -\cos\alpha[-T\cos\lambda + m(a_x - g_x)]$$
$$+ \sin\alpha[-T\sin\lambda + m(a_z - g_z)] \tag{9}$$

Equivalent small-angle expressions are

$$L = m[\alpha(a_x - g_x) + (a_z - g_z)] - T(\alpha + \lambda) \tag{10}$$

and

$$D = T - m[(a_x - g_x) - \alpha(a_z - g_z)] \tag{11}$$

where the angles are in radians.

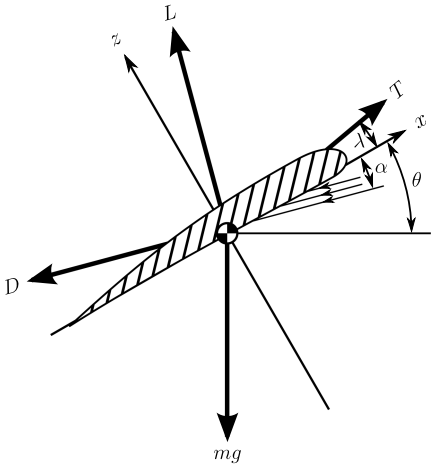

Fig. 1 Aerodynamic forces and angles.

Turbulence

Atmospheric turbulence is conventionally modeled as filtered Gaussian white noise. The longitudinal, lateral, and vertical components are modeled independently. The Dryden turbulence model is one commonly used atmospheric turbulence model [31]. It specifies the spectra of the three components as follows:

$$\Phi_{u_g}(\Omega) = \sigma_u^2 \frac{2L_u}{\pi}\frac{1}{1 + (L_u\Omega)^2} \tag{12a}$$

$$\Phi_{v_g}(\Omega) = \sigma_v^2 \frac{L_v}{\pi}\frac{1 + 3(L_v\Omega)^2}{[1 + (L_v\Omega)^2]^2} \tag{12b}$$

$$\Phi_{w_g}(\Omega) = \sigma_w^2 \frac{L_w}{\pi}\frac{1 + 3(L_w\Omega)^2}{[1 + (L_w\Omega)^2]^2} \tag{12c}$$

The spectra are given in terms of spatial frequency, which is converted to temporal frequency ω by multiplying by the speed of the aircraft,

$$\omega = \Omega U_0 \tag{13}$$

At medium to high altitudes (above 2000 ft), the turbulence is assumed to be isotropic. The characteristic lengths and the intensities in each direction are equal to each other. A typical characteristic length is 1750 ft. Intensities are charted as a function of altitude. Moderate turbulence has a root mean square intensity of about 10 ft/s at 2000 ft, decreasing roughly linearly to near 0 at 60,000 ft.

Whereas the lateral turbulence has little effect on the speed of an aircraft, the longitudinal turbulence has a direct effect on the airspeed. The longitudinal turbulence with a spectrum matching that given in Eq. (12a) can be obtained by passing white noise through a filter of the form

$$\sigma_u\sqrt{\frac{2L_u}{U_0}}\frac{1}{(L_u/U_0)s + 1} \tag{14}$$

The vertical turbulence could be simulated by passing white noise through a filter of the form

$$\sigma_w\sqrt{\frac{L_w}{U_0}}\frac{1 + \sqrt{3}(L_w/U_0)s}{[1 + (L_w/U_0)s]^2} \tag{15}$$

but for simplicity, this can be approximated as

$$\sigma_w\sqrt{\frac{L_w}{U_0}}\frac{1}{1 + (L_w/U_0)s} \tag{16}$$

Control Law

The equations required to implement the extremum-seeking control law are as follows:

$$\hat{f} \triangleq s_1 + s_2(U - V_{\text{cmd}}) + s_3(V - V_{\text{cmd}}) \tag{17a}$$

$$\dot{s}_1 = k_1(f - \hat{f}) + (s_2 + s_3)\dot{V}_{\text{cmd}} \tag{17b}$$

$$\dot{s}_2 = k_2(U - V_{\text{cmd}})(f - \hat{f}) + \sigma_2\dot{V}_{\text{cmd}} \tag{17c}$$

$$\dot{s}_3 = k_3(V - V_{\text{cmd}})(f - \hat{f}) + \sigma_3\dot{V}_{\text{cmd}} \tag{17d}$$

$$\dot{V}_{\text{cmd}} = k_{\text{ES}}(s_2 + s_3) \tag{17e}$$

where

$$f \triangleq \frac{L}{D} \approx \frac{m[\alpha(a_x - g_x) + (a_z - g_z)] - T(\alpha + \lambda)}{T - m[(a_x - g_x) - \alpha(a_z - g_z)]} \tag{18a}$$

$$U \triangleq V\sqrt{\frac{mg}{L}} \approx V\sqrt{\frac{mg}{m[\alpha(a_x - g_x) + (a_z - g_z)] - T(\alpha + \lambda)}} \tag{18b}$$

Details and motivations will be provided over the next several paragraphs.The control law is a four-state nonlinear controller that provides as its output an airspeed command, V_{cmd}, to an inner-loop airspeed controller (which is assumed to already be in place). The inputs to the control law are the lift to drag ratio f, airspeed V, and equivalent steady-state airspeed U. These inputs can be calculated from the following measured or approximated quantities: angle of attack α, engine thrust T, aircraft mass m, longitudinal and vertical body-axis accelerometer readings $(a_x - g_x)$ and $(a_z - g_z)$, thrust angle λ, acceleration due to gravity g, and airspeed V. Small-angle approximations of f and U in terms of these quantities are given in Eq. (18). The control law design parameters are $k_1, k_2, k_3, k_{\text{ES}}, \sigma_2$, and σ_3. (Note that σ_2 and σ_3 have no relation to the rms turbulence intensities σ_u, σ_v, and σ_w.)

Loosely speaking, the control law operates by determining a measurement of the lift to drag ratio, determining if the lift to drag ratio improves with increasing or decreasing airspeed and adjusting the airspeed command until the highest possible lift to drag ratio is achieved. Conceptually, an estimator, excited by transients in the Mach number and angle of attack, then approximates the gradient of the lift to drag ratio. In level flight, a change in the Mach number is always accompanied by a change in the angle of attack, and so it is not possible to independently control both the airspeed and the angle of attack. The optimal speed is that which provides the maximum lift to drag ratio possible along a curve of constant lift in the angle of attack versus Mach number plane. A gradient ascent is performed to the optimal point.

Seeking to implement such a control law, though, a number of difficulties arise (not the least of which is that the nonlinear relationship between the angle of attack and the airspeed can destabilize the control system). It is advantageous to reformulate the lift to drag ratio as a function of two variables other than the angle of attack and the Mach number. As a basis for the function, the airspeed V is used in place of the Mach number. In place of the angle of attack, the equivalent steady-state airspeed U, defined as the airspeed required to produce an amount of lift equal to the weight of the aircraft while in flight at the current coefficients of lift and altitude, is used. The estimator approximates the gradient of the lift to drag ratio in the U-V plane. When the lift produced by the aircraft is equal to its weight, U is equal to V, and so, in the U-V plane, the curve of constant lift is simply $U = V$. Based on the estimated gradient, the control law performs a gradient ascent along this line towards the speed at which the maximum lift to drag ratio is achieved.

The extremum-seeking algorithm is designed to use naturally occurring disturbances such as atmospheric turbulence to provide sufficient excitation to the estimator. The intensity of the turbulence is of course not known or constant; neither are the relative intensities of the vertical component of turbulence (affecting U) and the horizontal component (affecting V). In such a situation, a standard extremum-seeking algorithm (which estimates the slope by demodulating the lift to drag ratio with U and V) produces slope estimates that are proportional to the true slope, but the estimates are scaled by the square of the amplitudes of the vertical and horizontal components of turbulence, respectively. If the two slope estimates are scaled differently, the estimated slope along the line of constant lift cannot be determined. Because of this, the control algorithm uses a gradient estimator that is different from those commonly used in extremum seeking.

The gradient estimator is based on an estimate of the lift to drag ratio at the current U and V. The estimate is linear in the three estimator states, with the first state s_1 representing the lift to drag ratio at the commanded airspeed in steady flight, the second state s_2 representing the slope of the lift to drag ratio with U, and the third state s_3 representing the slope with respect to V. The states are updated based on the difference between the measured and estimated lift to drag ratios, f and $\hat{f}$. The slope of the lift to drag ratio along the line of constant lift is the sum of the second and third estimator states, s_2 and s_3, and the airspeed command is changed at a rate proportional to this slope. (The simplicity seen in this calculation of the slope along the line of constant lift is part of the motivation for reformulating f as a function of U and V. Calculating the slope along the curve of constant lift in the angle of attack versus Mach number plane is less than straightforward; the direction of a line tangent to the curve cannot be found without assuming knowledge of the rate of change of C_L with α, and the fundamental goal of extremum seeking is to perform an optimization without making assumptions about the aerodynamic characteristics of the aircraft.)

Note that several terms not related to the estimation error appear in the estimator equations. These terms [the last terms in Eqs. (17b–17d)] improve the transient performance by providing an estimate of how the estimator states are expected to change based on the rate of change of the airspeed command. As is shown in the following analysis, this also has a positive effect on stability of the algorithm. These terms are motivated by the expected change in the estimator states given a change in V_{cmd}. For example, $[(s_2 + s_3)\dot{V}_{\text{cmd}}]$ can be thought of as $[(f_U + f_V)\dot{V}_{\text{cmd}}]$ or $[(\mathrm{d}f/\mathrm{d}V_{\text{cmd}})\dot{V}_{\text{cmd}}]$, which is $\dot{f}$. This provides a sort of feedforward to s_1 (which is the estimate of f) when V_{cmd} changes. The terms in the $\dot{s}_2$ and $\dot{s}_3$ equations are similarly motivated. In this way, the design parameters σ_2 and σ_3 can be thought of as a priori estimates of $\mathrm{d}f_U/\mathrm{d}V_{\text{cmd}}$ and $\mathrm{d}f_V/\mathrm{d}V_{\text{cmd}}$, respectively.

Finally, a note about the order of the controller may be appropriate. The controller estimates a gradient in two dimensions for what is essentially a one-dimensional optimization. It is tempting to reformulate the problem as a one-dimensional optimization in one dimension so that the order of the gradient estimator can be reduced. Specifically, the gradient estimator could replace the two states s_2 and s_3 (which estimate f_U and f_V, respectively) with one state (say, s_{2+3}) that directly estimates the sum $f_U + f_V$. Such a controller could be derived by defining $s_{2+3} \triangleq s_2 + s_3$ and $s_{2-3} \triangleq s_2 - s_3$, rewriting the controller in terms of these new variables and dropping all terms containing s_{2-3}. This would be possible because the new update law ($\dot{V}_{\text{cmd}} = k_{\text{ES}}s_{2+3}$) would not depend on s_{2-3}. Furthermore, the expectation would be that disturbances accounted for by s_{2-3} in the estimate of the lift to drag ratio $\hat{f}$ would average to zero and could be ignored.

The problem is that disturbances in $(U + V)$ are likely to be strongly correlated with disturbances in $(U - V)$. This is the case even if it is assumed that U is not correlated with V because the amplitudes of the disturbances in U and V are not the same size; in general, disturbances in U are larger than disturbances in V, even in isotropic turbulence (and given two uncorrelated random variables, their sum is correlated with their difference unless their variances are equal). Although not presented in this paper, it can be shown through analysis that this correlation causes a bias in the estimate of the optimal endurance speed. Estimating the gradient in two dimensions, rather than one, removes this source of bias.

Analysis

For the analysis, assume that measurements of f, U, and V are available, and implement the control law given in Eq. (17). Let f be a static map in two dimensions. Assume that along the curve where the lift equals the weight of the aircraft, the map is convex. Assume stochastic perturbations in U and V that are each represented by filtered white noise. These stochastic perturbations approximate the longitudinal and vertical components of the turbulence. Under these assumptions, U and V are

$$\epsilon_1 \mathrm{d}\eta_1 = -\eta_1 \mathrm{d}t + \sqrt{\epsilon_1} q_1 \mathrm{d}W_1 \tag{19a}$$

$$\Delta U = a_1 \mathrm{sat}\eta_1 \tag{19b}$$

$$U = v + \Delta U \tag{19c}$$

$$\epsilon_2 \mathrm{d}\eta_2 = -\eta_2 \mathrm{d}t + \sqrt{\epsilon_2} q_2 \mathrm{d}W_2 \tag{20a}$$

$$\Delta V = a_2 \mathrm{sat}\eta_2 \tag{20b}$$

$$V = v + \Delta V \tag{20c}$$

The saturation function is defined as

$$\mathrm{sat}(\eta) = \begin{cases} \eta & \text{if } -1 < \eta < 1 \\ 1 & \text{if } \eta \geq 1 \\ -1 & \text{if } \eta \leq -1 \end{cases} \tag{21}$$

It is included primarily for mathematical convenience but also conveys the fact that real turbulence has a finite amplitude. Approximate the aircraft's control over the airspeed using simple first-order dynamics,

$$\dot{v} = \frac{1}{\tau}(V_{\mathrm{cmd}} - V) \tag{22}$$

This simple aircraft model is used to limit the order of the system being analyzed; other aircraft dynamics are subsumed in the stochastic perturbations to U and V. The time constant involved in the aircraft's control over the airspeed is explicitly modeled because the analysis in [1] showed it to have possible implications for stability.

With these models, the closed-loop system is

$$\dot{v} = \frac{1}{\tau}(V_{\mathrm{cmd}} - v - a_2 \mathrm{sat}\eta_2) \tag{23a}$$

$$\begin{aligned}\dot{s}_1 = {} & k_1(f - s_1 - s_2(v + a_1 \mathrm{sat}\eta_1 - V_{\mathrm{cmd}}) \\ & - s_3(v + a_2 \mathrm{sat}\eta_2 - V_{\mathrm{cmd}})) + (s_2 + s_3)\dot{V}_{\mathrm{cmd}}\end{aligned} \tag{23b}$$

$$\begin{aligned}\dot{s}_2 = {} & k_2(v + a_1 \mathrm{sat}\eta_1 - V_{\mathrm{cmd}}) \times (f - s_1 - s_2(v + a_1 \mathrm{sat}\eta_1 - V_{\mathrm{cmd}}) \\ & - s_3(v + a_2 \mathrm{sat}\eta_2 - V_{\mathrm{cmd}})) + \sigma_2 \dot{V}_{\mathrm{cmd}}\end{aligned} \tag{23c}$$

$$\begin{aligned}\dot{s}_3 = {} & k_3(v + a_2 \mathrm{sat}\eta_2 - V_{\mathrm{cmd}}) \times (f - s_1 - s_2(v + a_1 \mathrm{sat}\eta_1 - V_{\mathrm{cmd}}) \\ & - s_3(v + a_2 \mathrm{sat}\eta_2 - V_{\mathrm{cmd}})) + \sigma_3 \dot{V}_{\mathrm{cmd}}\end{aligned} \tag{23d}$$

$$\dot{V}_{\mathrm{cmd}} = k_{\mathrm{ES}}(s_2 + s_3) \tag{23e}$$

$$\epsilon_1 \mathrm{d}\eta_1 = -\eta_1 \mathrm{d}t + \sqrt{\epsilon_1} q_1 \mathrm{d}W_1 \tag{23f}$$

$$\epsilon_2 \mathrm{d}\eta_2 = -\eta_2 \mathrm{d}t + \sqrt{\epsilon_2} q_2 \mathrm{d}W_2 \tag{23g}$$

It is this closed-loop system that is considered in the following analysis.

Theorem 1: Consider system (23), where $f = f(U, V) = f(v + a_1 \mathrm{sat}\eta_1, v + a_2 \mathrm{sat}\eta_2)$ is a two-dimensional map that, along the line $V = U$, is convex with a maximum at (V_*, V_*). Assume all constants are positive, with the exception of σ_2 and σ_3, which are chosen so that $\sigma_3 < \frac{1}{2}(f_{VV*} - f_{UU*})$ and $\sigma_2 < \frac{1}{2}(f_{UU*} - f_{VV*})$. Let constants C_2 and C_4 be defined by

$$C_2(q_i) \triangleq \frac{q_i^2}{2} \mathrm{erf}\frac{1}{q_i} - \frac{q_i}{\sqrt{\pi}} e^{\frac{-1}{q_i^2}} + 1 - \mathrm{erf}\frac{1}{q_i} \tag{24a}$$

$$C_4(q_i) \triangleq \frac{3}{4} q_i^4 \mathrm{erf}\frac{1}{q_i} - \frac{q_i}{\sqrt{\pi}} e^{\frac{-1}{q_i^2}}\left(1 + \frac{3}{2} q_i^2\right) + 1 - \mathrm{erf}\frac{1}{q_i} \tag{24b}$$

Suppose $f(U, V)$ is three times differentiable at (V_*, V_*). Then, there exists a constant a^* such that for any $0 < (a_1, a_2) < a^*$ there exist constants $r > 0$, $c > 0$, $\gamma > 0$, and a function $T(\epsilon_1, \epsilon_2) : (0, \epsilon_0) \times (0, \epsilon_0) \to \mathbb{N}$ with the property $\lim_{\epsilon_1, \epsilon_2 \to 0} T(\epsilon_1, \epsilon_2) = \infty$ such that for any initial condition $|\Delta^{\epsilon,a}(0)| < r$ and any $\delta > 0$,

$$\begin{aligned}\lim_{\epsilon_1, \epsilon_2 \to 0} \inf\{t \geq 0 : {} & |\Delta^{\epsilon,a}(t)| > c|\Delta^{\epsilon,a}(0)|e^{-\gamma t} + O(a_1^4 a_2^{-1}) + O(a_1^3) \\ & + O(a_1^2 a_2) + O(a_1 a_2^2) + O(a_2^3) + O(a_1^{-1} a_2^4) + \delta\} = \infty, \text{ a.s.}\end{aligned} \tag{25}$$

and

$$\begin{aligned}\lim_{\epsilon_1, \epsilon_2 \to 0} P\{ & |\Delta^{\epsilon,a}(t)| \leq c|\Delta^{\epsilon,a}(0)|e^{-\gamma t} + O(a_1^4 a_2^{-1}) + O(a_1^3) + O(a_1^2 a_2) \\ & + O(a_1 a_2^2) + O(a_2^3) + O(a_1^{-1} a_2^4) + \delta, \quad \forall\, t \in [0, T(\epsilon_1, \epsilon_2)]\} = 1\end{aligned} \tag{26}$$

where

$$\Delta^{\epsilon,a}(t) \triangleq \begin{pmatrix} v(t) \\ s_1(t) \\ s_2(t) \\ s_3(t) \\ V_{\mathrm{cmd}}(t) \end{pmatrix} - \begin{pmatrix} \bar{v} \\ \bar{s}_1 \\ \bar{s}_2 \\ \bar{s}_3 \\ \bar{V}_{\mathrm{cmd}} \end{pmatrix}$$

and

$$\begin{aligned}\bar{v} = {} & V_* - \frac{f_{UUU^*} C_4(q_1) + 3 f_{UUV^*}(C_2(q_1))^2}{6(f_{UU^*} + 2f_{UV^*} + f_{VV^*}) C_2(q_1)} a_1^2 \\ & - \frac{3 f_{UVV^*}(C_2(q_2))^2 + f_{VVV^*} C_4(q_2)}{6(f_{UU^*} + 2f_{UV^*} + f_{VV^*}) C_2(q_2)} a_2^2\end{aligned} \tag{27a}$$

$$\bar{s}_1 = f_* + \frac{1}{2}[f_{UU^*} a_1^2 C_2(q_1) + f_{VV^*} a_2^2 C_2(q_2)] \tag{27b}$$

$$\begin{aligned}\bar{s}_2 = {} & f_{U^*} - (f_{UU^*} + f_{UV^*}) \\ & \times \left[\frac{f_{UUU^*} C_4(q_1) + 3 f_{UUV^*}(C_2(q_1))^2}{6(f_{UU^*} + 2f_{UV^*} + f_{VV^*}) C_2(q_1)} a_1^2 \right. \\ & \left. + \frac{3 f_{UVV^*}(C_2(q_2))^2 + f_{VVV^*} C_4(q_2)}{6(f_{UU^*} + 2f_{UV^*} + f_{VV^*}) C_2(q_2)} a_2^2\right] \\ & + \frac{1}{6} f_{UUU^*} a_1^2 \frac{C_4(q_1)}{C_2(q_1)} + \frac{1}{2} f_{UVV^*} a_2^2 C_2(q_2)\end{aligned} \tag{27c}$$

$$\bar{s}_3 = f_{V^*} - (f_{UV^*} + f_{VV^*}) \times \left[\frac{f_{UUV^*}C_4(q_1) + 3f_{UUV^*}(C_2(q_1))^2}{6(f_{UU^*} + 2f_{UV^*} + f_{VV^*})C_2(q_1)}a_1^2 + \frac{3f_{UVV^*}(C_2(q_2))^2 + f_{VVV^*}C_4(q_2)}{6(f_{UU^*} + 2f_{UV^*} + f_{VV^*})C_2(q_2)}a_2^2\right] + \frac{1}{2}f_{UUV^*}a_1^2C_2(q_1) + \frac{1}{6}f_{VVV^*}a_2^2\frac{C_4(q_2)}{C_2(q_2)} \tag{27d}$$

$$\bar{V}_{\text{cmd}} = V_* - \frac{f_{UUU^*}C_4(q_1) + 3f_{UUV^*}(C_2(q_1))^2}{6(f_{UU^*} + 2f_{UV^*} + f_{VV^*})C_2(q_1)}a_1^2 - \frac{3f_{UVV^*}(C_2(q_2))^2 + f_{VVV^*}C_4(q_2)}{6(f_{UU^*} + 2f_{UV^*} + f_{VV^*})C_2(q_2)}a_2^2 \tag{27e}$$

Theorem 1 roughly states that the stochastic system converges on average to the airspeed for optimal endurance, with a bias that is proportional to the square of the turbulence intensity and the third partial derivatives of the lift to drag ratio map. (Mathematically speaking, the system converges both almost surely and in probability.) The theorem concerns the system behavior for small turbulence intensities and for timescales that are long compared to the turbulence time constants.

Proof of Theorem

The average system is formed by performing stochastic averaging over the invariant distributions of η_1 and η_2. The distributions of the stochastic variables are given by

$$\mu(\mathrm{d}\eta) = \frac{1}{\sqrt{\pi}q}e^{-(\eta^2/q^2)}\mathrm{d}\eta \tag{28}$$

where the appropriate subscript is to be appended to η and q. Note that

$$\int_{-\infty}^{\infty}\mu(\mathrm{d}\eta) = 1 \tag{29}$$

$$\int_{-\infty}^{\infty}(\mathrm{sat}\eta)^k\mu(\mathrm{d}\eta) = 0 \quad \text{for k} = 1, 3, 5, \ldots \tag{30}$$

$$\int_{-\infty}^{\infty}(\mathrm{sat}\eta)^2\mu(\mathrm{d}\eta) = C_2(q) \tag{31}$$

$$\int_{-\infty}^{\infty}(\mathrm{sat}\eta)^4\mu(\mathrm{d}\eta) = C_4(q) \tag{32}$$

Taking $\dot{v}$ as an example, averaging over both stochastic variables gives

$$\dot{v} = \int_{-\infty}^{\infty}\int_{-\infty}^{\infty}\frac{1}{\tau}(V_{\text{cmd}} - v - a_2\mathrm{sat}\eta_2)\mu(\mathrm{d}\eta_1)\mu(\mathrm{d}\eta_2) = \int_{-\infty}^{\infty}\frac{1}{\tau}(V_{\text{cmd}} - v - a_2\mathrm{sat}\eta_2)\mu(\mathrm{d}\eta_2) = \frac{1}{\tau}(V_{\text{cmd}} - v) \tag{33}$$

After performing similar averaging on all dynamic equations, the average system is

$$\dot{v} = \frac{1}{\tau}(V_{\text{cmd}} - v) \tag{34a}$$

$$\dot{s}_1 = k_1\left(\int_{-\infty}^{\infty}\int_{-\infty}^{\infty}f\mu(\mathrm{d}\eta_1)\mu(\mathrm{d}\eta_2) - s_1 - s_2(v - V_{\text{cmd}}) - s_3(v - V_{\text{cmd}})\right) + (s_2 + s_3)\dot{V}_{\text{cmd}} \tag{34b}$$

$$\dot{s}_2 = k_2(v - V_{\text{cmd}}) \times \left(\int_{-\infty}^{\infty}\int_{-\infty}^{\infty}f\mu(\mathrm{d}\eta_1)\mu(\mathrm{d}\eta_2) - s_1 - s_2(v - V_{\text{cmd}}) - s_3(v - V_{\text{cmd}})\right) + k_2\left(\int_{-\infty}^{\infty}\int_{-\infty}^{\infty}a_1\mathrm{sat}\eta_2 f\mu(\mathrm{d}\eta_1)\mu(\mathrm{d}\eta_2) - s_2a_1^2C_2(q_1)\right) + \sigma_2\dot{V}_{\text{cmd}} \tag{34c}$$

$$\dot{s}_3 = k_3(v - V_{\text{cmd}}) \times \left(\int_{-\infty}^{\infty}\int_{-\infty}^{\infty}f\mu(\mathrm{d}\eta_1)\mu(\mathrm{d}\eta_2) - s_1 - s_2(v - V_{\text{cmd}}) - s_3(v - V_{\text{cmd}})\right) + k_3\left(\int_{-\infty}^{\infty}\int_{-\infty}^{\infty}a_2\mathrm{sat}\eta_2 f\mu(\mathrm{d}\eta_1)\mu(\mathrm{d}\eta_2) - s_3a_2^2C_2(q_2)\right) + \sigma_3\dot{V}_{\text{cmd}} \tag{34d}$$

$$\dot{V}_{\text{cmd}} = k_{\text{ES}}(s_2 + s_3) \tag{34e}$$

At equilibrium, setting the time derivatives to zero and assuming nonzero constants, the system of equations reduces to

$$0 = V_{\text{cmd}} - v \tag{35a}$$

$$0 = \int_{-\infty}^{\infty}\int_{-\infty}^{\infty}f\mu(\mathrm{d}\eta_1)\mu(\mathrm{d}\eta_2) - s_1 \tag{35b}$$

$$0 = \int_{-\infty}^{\infty}\int_{-\infty}^{\infty}a_1\mathrm{sat}\eta_1 f\mu(\mathrm{d}\eta_1)\mu(\mathrm{d}\eta_2) - s_2a_1^2C_2(q_1) \tag{35c}$$

$$0 = \int_{-\infty}^{\infty}\int_{-\infty}^{\infty}a_2\mathrm{sat}\eta_2 f\mu(\mathrm{d}\eta_1)\mu(\mathrm{d}\eta_2) - s_3a_2^2C_2(q_2) \tag{35d}$$

$$0 = s_2 + s_3 \tag{35e}$$

To evaluate the integrals in question, take a two-dimensional Taylor expansion of v in a_1 and a_2,

$$v = n_0 + [n_1a_1 + n_2a_2] + [n_{11}a_1^2 + n_{12}a_1a_2 + n_{22}a_2^2] + [n_{111}a_1^3 + n_{112}a_1^2a_2 + n_{122}a_1a_2^2 + n_{222}a_2^3] + O(a_1^4) + O(a_1^3a_2) + O(a_1^2a_2^2) + O(a_1a_2^3) + O(a_2^4) \tag{36}$$

Note that U and V can be expressed in terms of v,

$$U = v + a_1\mathrm{sat}\eta_1 \tag{37a}$$

$$V = v + a_2\mathrm{sat}\eta_2 \tag{37b}$$

Then,

$$U = n_0 + [n_1a_1 + n_2a_2] + [n_{11}a_1^2 + n_{12}a_1a_2 + n_{22}a_2^2] + [n_{111}a_1^3 + n_{112}a_1^2a_2 + n_{122}a_1a_2^2 + n_{222}a_2^3] + a_1\mathrm{sat}\eta_1 + O(a_1^4) + O(a_1^3a_2) + O(a_1^2a_2^2) + O(a_1a_2^3) + O(a_2^4) \tag{38}$$

$$V = n_0 + [n_1a_1 + n_2a_2] + [n_{11}a_1^2 + n_{12}a_1a_2 + n_{22}a_2^2] + [n_{111}a_1^3 + n_{112}a_1^2a_2 + n_{122}a_1a_2^2 + n_{222}a_2^3] + a_2\mathrm{sat}\eta_2 + O(a_1^4) + O(a_1^3a_2) + O(a_1^2a_2^2) + O(a_1a_2^3) + O(a_2^4) \tag{39}$$

Use these expressions in a two-dimensional Taylor expansion of f, which is a function of U and V. Let the expansion be centered at the

point (n_0, n_0). The notation f_0 is used to mean the value of the lift to drag ratio at this point. Similarly, f_{U0} is used to mean the partial derivative of the lift to drag ratio with respect to U at the same point; f_{V0} is the partial derivative with respect to V; f_{UV0} and similar denote higher partial derivatives. The expansion of f is

$$\begin{aligned} f = {} & f_0 + [f_{U0}(U-n_0) + f_{V0}(V-n_0)] + \frac{1}{2}[f_{UU0}(U-n_0)^2 \\ & + 2f_{UV0}(U-n_0)(V-n_0) + f_{VV0}(V-n_0)^2] \\ & + \frac{1}{3!}[f_{UUU0}(U-n_0)^3 + 3f_{UUV0}(U-n_0)^2(V-n_0) \\ & + 3f_{UVV0}(U-n_0)(V-n_0)^2 + f_{VVV0}(V-n_0)^3] \\ & + O((U-n_0)^4) + O((U-n_0)^3(V-n_0)) \\ & + O((U-n_0)^2(V-n_0)^2) + O((U-n_0)(V-n_0)^3) \\ & + O((V-n_0)^4) \end{aligned} \tag{40}$$

The expression $(U-n_0)$ simplifies by the cancellation of the n_0 terms to the following:

$$\begin{aligned} U - n_0 = {} & [n_1a_1 + n_2a_2] + [n_{11}a_1^2 + n_{12}a_1a_2 + n_{22}a_2^2] \\ & + [n_{111}a_1^3 + n_{112}a_1^2a_2 + n_{122}a_1a_2^2 + n_{222}a_2^3] + a_1\mathrm{sat}\eta_1 \\ & + O(a_1^4) + O(a_1^3a_2) + O(a_1^2a_2^2) + O(a_1a_2^3) + O(a_2^4) \end{aligned} \tag{41}$$

Note that

$$O(U-n_0) = O(a_1) + O(a_2) \tag{42}$$

Similarly,

$$\begin{aligned} V - n_0 = {} & [n_1a_1 + n_2a_2] + [n_{11}a_1^2 + n_{12}a_1a_2 + n_{22}a_2^2] \\ & + [n_{111}a_1^3 + n_{112}a_1^2a_2 + n_{122}a_1a_2^2 + n_{222}a_2^3] + a_2 sat\eta_2 \\ & + O(a_1^4) + O(a_1^3a_2) + O(a_1^2a_2^2) + O(a_1a_2^3) + O(a_2^4) \end{aligned} \tag{43}$$

and

$$O(V-n_0) = O(a_1) + O(a_2) \tag{44}$$

Substituting the Taylor expansions of U and V into the expansion of f and simplifying gives

$$\begin{aligned} f = {} & f_0 + [f_{U0}([n_1a_1 + n_2a_2] + [n_{11}a_1^2 + n_{12}a_1a_2 + n_{22}a_2^2] \\ & + [n_{111}a_1^3 + n_{112}a_1^2a_2 + n_{122}a_1a_2^2 + n_{222}a_2^3] + a_1\mathrm{sat}\eta_1) \\ & + f_{V0}([n_1a_1 + n_2a_2] + [n_{11}a_1^2 + n_{12}a_1a_2 + n_{22}a_2^2] \\ & + [n_{111}a_1^3 + n_{112}a_1^2a_2 + n_{122}a_1a_2^2 + n_{222}a_2^3] + a_2\mathrm{sat}\eta_2)] \\ & + \frac{1}{2}[f_{UU0}([n_1a_1 + n_2a_2] + [n_{11}a_1^2 + n_{12}a_1a_2 + n_{22}a_2^2] + a_1\mathrm{sat}\eta_1)^2 \\ & + 2f_{UV0}([n_1a_1 + n_2a_2] + [n_{11}a_1^2 + n_{12}a_1a_2 + n_{22}a_2^2] + a_1\mathrm{sat}\eta_1) \\ & \times([n_1a_1 + n_2a_2] + [n_{11}a_1^2 + n_{12}a_1a_2 + n_{22}a_2^2] + a_2\mathrm{sat}\eta_2) \\ & + f_{VV0}([n_1a_1 + n_2a_2] + [n_{11}a_1^2 + n_{12}a_1a_2 + n_{22}a_2^2] \\ & + a_2\mathrm{sat}\eta_2)^2] + \frac{1}{3!}[f_{UUU0}([n_1a_1 + n_2a_2] + a_1\mathrm{sat}\eta_1)^3 \\ & + 3f_{UUV0}([n_1a_1 + n_2a_2] + a_1\mathrm{sat}\eta_1)^2([n_1a_1 + n_2a_2] + a_2\mathrm{sat}\eta_2) \\ & + 3f_{UVV0}([n_1a_1 + n_2a_2] + a_1\mathrm{sat}\eta_1)([n_1a_1 + n_2a_2] + a_2\mathrm{sat}\eta_2)^2 \\ & + f_{VVV0}([n_1a_1 + n_2a_2] + a_2\mathrm{sat}\eta_2)^3] + O(a_1^4) \\ & + O(a_1^3a_2) + O(a_1^2a_2^2) + O(a_1a_2^3) + O(a_2^4) \end{aligned} \tag{45}$$

The integrals in Eq. (35) are then

$$\begin{aligned} & \int_{-\infty}^{\infty}\int_{-\infty}^{\infty} f\mu(\mathrm{d}\eta_1)\mu(\mathrm{d}\eta_2) = f_0 \\ & + [f_{U0}([n_1a_1 + n_2a_2] + [n_{11}a_1^2 + n_{12}a_1a_2 + n_{22}a_2^2] \\ & + [n_{111}a_1^3 + n_{112}a_1^2a_2 + n_{122}a_1a_2^2 + n_{222}a_2^3]) \\ & + f_{V0}([n_1a_1 + n_2a_2] + [n_{11}a_1^2 + n_{12}a_1a_2 + n_{22}a_2^2] \\ & + [n_{111}a_1^3 + n_{112}a_1^2a_2 + n_{122}a_1a_2^2 + n_{222}a_2^3])] \\ & + \frac{1}{2}[f_{UU0}([n_1a_1 + n_2a_2] + [n_{11}a_1^2 + n_{12}a_1a_2 + n_{22}a_2^2])^2 \\ & + a_1^2C_2(q_1)) + 2f_{UV0}([n_1a_1 + n_2a_2] \\ & + [n_{11}a_1^2 + n_{12}a_1a_2 + n_{22}a_2^2]) \\ & \times([n_1a_1 + n_2a_2] + [n_{11}a_1^2 + n_{12}a_1a_2 + n_{22}a_2^2]) \\ & + f_{VV0}([n_1a_1 + n_2a_2] + [n_{11}a_1^2 + n_{12}a_1a_2 + n_{22}a_2^2])^2 \\ & + a_2^2C_2(q_2))] + \frac{1}{3!}[f_{UUU0}([n_1a_1 + n_2a_2]^3 \\ & + 3[n_1a_1 + n_2a_2]a_1^2C_2(q_1)) + 3f_{UUV0}([n_1a_1 + n_2a_2]^2 \\ & + a_1^2C_2(q_1))([n_1a_1 + n_2a_2]) + 3f_{UVV0}([n_1a_1 + n_2a_2]) \\ & \times([n_1a_1 + n_2a_2] + a_2^2C_2(q_2)) + f_{VVV0}([n_1a_1 + n_2a_2]^3 \\ & + 3[n_1a_1 + n_2a_2]a_2^2C_2(q_2))] + O(a_1^4) + O(a_1^3a_2) \\ & + O(a_1^2a_2^2) + O(a_1a_2^3) + O(a_2^4) \end{aligned} \tag{46}$$

$$\begin{aligned} & \int_{-\infty}^{\infty}\int_{-\infty}^{\infty} a_1\mathrm{sat}\eta_1 f\mu(\mathrm{d}\eta_1)\mu(\mathrm{d}\eta_2) = [f_{U0}a_1^2C_2(q_1)] \\ & + \frac{1}{2}[f_{UU0}(2a_1^2C_2(q_1)([n_1a_1 + n_2a_2] + [n_{11}a_1^2 + n_{12}a_1a_2 + n_{22}a_2^2])) \\ & + 2f_{UV0}(a_1^2C_2(q_1))([n_1a_1 + n_2a_2] + [n_{11}a_1^2 + n_{12}a_1a_2 + n_{22}a_2^2])] \\ & + \frac{1}{3!}[f_{UUU0}([n_1a_1 + n_2a_2]^2a_1^2C_2(q_1) + a_1^4C_4(q_1)) \\ & + 3f_{UUV0}(2a_1^2C_2(q_1)[n_1a_1 + n_2a_2])([n_1a_1 + n_2a_2]) \\ & + 3f_{UVV0}(a_1^2C_2(q_1))([n_1a_1 + n_2a_2]^2 + a_2^2C_2(q_2))] \\ & + O(a_1^5) + O(a_1^4a_2) + O(a_1^3a_2^2) + O(a_1^2a_2^3) + O(a_1a_2^4) \\ & = f_{U0}a_1^2C_2(q_1) + f_{UU0}a_1^2C_2(q_1)([n_1a_1 + n_2a_2] \\ & + [n_{11}a_1^2 + n_{12}a_1a_2 + n_{22}a_2^2]) + f_{UV0}a_1^2C_2(q_1)([n_1a_1 + n_2a_2] \\ & + [n_{11}a_1^2 + n_{12}a_1a_2 + n_{22}a_2^2]) + \frac{1}{6}f_{UUU0}([n_1a_1 + n_2a_2]^2a_1^2C_2(q_1) \\ & + a_1^4C_4(q_1)) + f_{UUV0}a_1^2C_2(q_1)[n_1a_1 + n_2a_2]^2 \\ & + \frac{1}{2}f_{UVV0}a_1^2C_2(q_1)([n_1a_1 + n_2a_2]^2 + a_2^2C_2(q_2)) \\ & + O(a_1^5) + O(a_1^4a_2) + O(a_1^3a_2^2) + O(a_1^2a_2^3) + O(a_1a_2^4) \end{aligned} \tag{47}$$

$$\begin{aligned} & \int_{-\infty}^{\infty}\int_{-\infty}^{\infty} a_2\mathrm{sat}\eta_2 f\mu(\mathrm{d}\eta_1)\mu(\mathrm{d}\eta_2) = [f_{V0}a_2^2C_2(q_2)] \\ & + \frac{1}{2}[2f_{UV0}(a_2^2C_2(q_2))([n_1a_1 + n_2a_2] + [n_{11}a_1^2 + n_{12}a_1a_2 + n_{22}a_2^2] \\ & + f_{VV0}(2a_2^2C_2(q_2)([n_1a_1 + n_2a_2] + [n_{11}a_1^2 + n_{12}a_1a_2 + n_{22}a_2^2]))] \\ & + \frac{1}{3!}[3f_{UUV0}(a_2^2C_2(q_2))([n_1a_1 + n_2a_2]^2 + a_1^2C_2(q_1)) \\ & + 3f_{UVV0}(2a_2^2C_2(q_2)[n_1a_1 + n_2a_2])([n_1a_1 + n_2a_2]) \\ & + f_{VVV0}([n_1a_1 + n_2a_2]^2a_2^2C_2(q_2) + a_2^4C_4(q_2))] \\ & + O(a_1^4a_2) + O(a_1^3a_2^2) + O(a_1^2a_2^3) + O(a_1a_2^4) + O(a_2^5) \\ & = f_{V0}a_2^2C_2(q_2) + f_{UV0}a_2^2C_2(q_2)([n_1a_1 + n_2a_2] \\ & + [n_{11}a_1^2 + n_{12}a_1a_2 + n_{22}a_2^2]) + f_{VV0}a_2^2C_2(q_2)([n_1a_1 + n_2a_2] \\ & + [n_{11}a_1^2 + n_{12}a_1a_2 + n_{22}a_2^2]) + \frac{1}{2}f_{UUV0}a_2^2C_2(q_2)([n_1a_1 + n_2a_2]^2 \\ & + a_1^2C_2(q_1)) + f_{UVV0}a_2^2C_2(q_2)[n_1a_1 + n_2a_2]^2 \\ & + \frac{1}{6}f_{VVV0}([n_1a_1 + n_2a_2]^2a_2^2C_2(q_2) + a_2^4C_4(q_2)) + O(a_1^4a_2) \\ & + O(a_1^3a_2^2) + O(a_1^2a_2^3) + O(a_1a_2^4) + O(a_2^5) \end{aligned} \tag{48}$$

Solving Eqs. (35c) and (35d) for s_2 and s_3 gives

$$\begin{aligned}s_2 &= f_{U0} + f_{UU0}([n_1a_1 + n_2a_2] + [n_{11}a_1^2 + n_{12}a_1a_2 + n_{22}a_2^2]) \\ &+ f_{UV0}([n_1a_1 + n_2a_2] + [n_{11}a_1^2 + n_{12}a_1a_2 + n_{22}a_2^2]) \\ &+ \frac{1}{6}f_{UUU0}\left([n_1a_1 + n_2a_2]^2 + a_1^2\frac{C_4(q_1)}{C_2(q_1)}\right) \\ &+ f_{UUV0}[n_1a_1 + n_2a_2]^2 + \frac{1}{2}f_{UVV0}([n_1a_1 + n_2a_2]^2 \\ &+ a_2^2C_2(q_2)) + O(a_1^3) + O(a_1^2a_2) + O(a_1a_2^2) \\ &+ O(a_2^3) + O(a_1^{-1}a_2^4)\end{aligned} \tag{49}$$

$$\begin{aligned}s_3 &= f_{V0} + f_{UV0}([n_1a_1 + n_2a_2] + [n_{11}a_1^2 + n_{12}a_1a_2 + n_{22}a_2^2]) \\ &+ f_{VV0}([n_1a_1 + n_2a_2] + [n_{11}a_1^2 + n_{12}a_1a_2 + n_{22}a_2^2]) \\ &+ \frac{1}{2}f_{UUV0}([n_1a_1 + n_2a_2]^2 + a_1^2C_2(q_1)) + f_{UVV0}[n_1a_1 + n_2a_2]^2 \\ &+ \frac{1}{6}f_{VVV0}\left([n_1a_1 + n_2a_2]^2 + a_2^2\frac{C_4(q_2)}{C_2(q_2)}\right) + O(a_1^4a_2^{-1}) \\ &+ O(a_1^3) + O(a_1^2a_2) + O(a_1a_2^2) + O(a_2^3)\end{aligned} \tag{50}$$

Substituting these expressions into Eq. (35e) gives

$$\begin{aligned}0 &= f_{U0} + f_{V0} + (f_{UU0} + 2f_{UV0} + f_{VV0})([n_1a_1 + n_2a_2] \\ &+ [n_{11}a_1^2 + n_{12}a_1a_2 + n_{22}a_2^2]) \\ &+ \frac{1}{6}f_{UUU0}\left([n_1a_1 + n_2a_2]^2 + a_1^2\frac{C_4(q_1)}{C_2(q_1)}\right) \\ &+ \frac{1}{2}f_{UUV0}(3[n_1a_1 + n_2a_2]^2 + a_1^2C_2(q_1)) \\ &+ \frac{1}{2}f_{UVV0}(3[n_1a_1 + n_2a_2]^2 + a_2^2C_2(q_2)) \\ &+ \frac{1}{6}f_{VVV0}\left([n_1a_1 + n_2a_2]^2 + a_2^2\frac{C_4(q_2)}{C_2(q_2)}\right) + O(a_1^4a_2^{-1}) \\ &+ O(a_1^3) + O(a_1^2a_2) + O(a_1a_2^2) + O(a_2^3) + O(a_1^{-1}a_2^4)\end{aligned} \tag{51}$$

This equation is a polynomial in a_1 and a_2, and so, for the expression to be equal to zero the coefficients of each power of a must each be zero. Equating coefficients gives

$$a^0{:}0 = f_{U0} + f_{V0} \tag{52a}$$

$$a_1^1{:}0 = (f_{UU0} + 2f_{UV0} + f_{VV0})n_1 \tag{52b}$$

$$a_2^1{:}0 = (f_{UU0} + 2f_{UV0} + f_{VV0})n_2 \tag{52c}$$

$$\begin{aligned}a_1^2{:}0 &= (f_{UU0} + 2f_{UV0} + f_{VV0})n_{11} + \frac{1}{6}f_{UUU0}\left(n_1^2 + \frac{C_4(q_1)}{C_2(q_1)}\right) \\ &+ \frac{1}{2}f_{UUV0}(3n_1^2 + C_2(q_1)) + \frac{1}{2}f_{UVV0}(3n_1^2) + \frac{1}{6}f_{VVV0}(n_1^2)\end{aligned} \tag{52d}$$

$$\begin{aligned}a_1a_2{:}0 &= (f_{UU0} + 2f_{UV0} + f_{VV0})n_{12} + \frac{1}{6}f_{UUU0}(2n_1n_2) \\ &+ \frac{1}{2}f_{UUV0}(6n_1n_2) + \frac{1}{2}f_{UVV0}(6n_1n_2) + \frac{1}{6}f_{VVV0}(2n_1n_2)\end{aligned} \tag{52e}$$

$$\begin{aligned}a_2^2{:}0 &= (f_{UU0} + 2f_{UV0} + f_{VV0})n_{22} + \frac{1}{6}f_{UUU0}(n_2^2) + \frac{1}{2}f_{UUV0}(3n_2^2) \\ &+ \frac{1}{2}f_{UVV0}(3n_2^2 + C_2(q_2)) + \frac{1}{6}f_{VVV0}\left(n_2^2 + \frac{C_4(q_2)}{C_2(q_2)}\right)\end{aligned} \tag{52f}$$

At this point, consider the nature of the map. In steady flight, the aircraft is confined to the line $U = V$. Therefore, the optimal airspeed, which we will denote by V_*, is that point at which the component of the gradient in the direction of that line is zero. That is,

$$\left.\frac{\partial f}{\partial U}\right|_{V_*} + \left.\frac{\partial f}{\partial V}\right|_{V_*} = f_{U*} + f_{V*} = 0 \tag{53}$$

Recall that the f_0 notation concerns the lift to drag ratio at the point (n_0, n_0). Assuming that, along the line $U = V$ the map has a unique maximum, the a^0 equation requires that

$$n_0 = V_* \tag{54}$$

If the maximum is unique, then the curvature at that point along the line $U = V$ is nonzero (specifically, negative). The curvature along this line is

$$\begin{aligned}&\frac{\partial}{\partial U}\left[\frac{\partial f}{\partial U} + \frac{\partial f}{\partial V}\right]\Bigg|_{V_*} + \frac{\partial}{\partial V}\left[\frac{\partial f}{\partial U} + \frac{\partial f}{\partial V}\right]\Bigg|_{V_*} \\ &\quad = \left.\frac{\partial^2 f}{(\partial U)^2}\right|_{V_*} + 2\left.\frac{\partial^2 f}{\partial U\partial V}\right|_{V_*} + \left.\frac{\partial^2 f}{(\partial V)^2}\right|_{V_*} \\ &\quad = f_{UU*} + 2f_{UV*} + f_{VV*} < 0\end{aligned} \tag{55}$$

Because $n_0 = V_*$, this means that f_0 is the same as f_*, and all derivatives are the same as well. Because the quantity in Eq. (55) is negative and therefore nonzero, it can be divided out of Eqs. (52b) and (52c) to give

$$n_1 = 0 \tag{56}$$

$$n_2 = 0 \tag{57}$$

This simplifies the remaining equations in Eq. (52). They become

$$\begin{aligned}a_1^2{:}0 &= (f_{UU*} + 2f_{UV*} + f_{VV*})n_{11} \\ &+ \frac{1}{6}f_{UUU*}\frac{C_4(q_1)}{C_2(q_1)} + \frac{1}{2}f_{UUV*}C_2(q_1)\end{aligned} \tag{58a}$$

$$a_1a_2{:}0 = (f_{UU*} + 2f_{UV*} + f_{VV*})n_{12} \tag{58b}$$

$$\begin{aligned}a_2^2{:}0 &= (f_{UU*} + 2f_{UV*} + f_{VV*})n_{22} + \frac{1}{2}f_{UVV*}C_2(q_2) \\ &+ \frac{1}{6}f_{VVV*}\frac{C_4(q_2)}{C_2(q_2)}\end{aligned} \tag{58c}$$

which gives

$$n_{11} = -\frac{f_{UUU*}C_4(q_1) + 3f_{UUV*}(C_2(q_1))^2}{6(f_{UU*} + 2f_{UV*} + f_{VV*})C_2(q_1)} \tag{59}$$

$$n_{12} = 0 \tag{60}$$

$$n_{22} = -\frac{3f_{UVV*}(C_2(q_2))^2 + f_{VVV*}C_4(q_2)}{6(f_{UU*} + 2f_{UV*} + f_{VV*})C_2(q_2)} \tag{61}$$

Substituting the obtained values of n_0, n_1, n_2, n_{11}, n_{12}, and n_{22} back into the original Taylor expansion (36) gives a second-order expression for the equilibrium value of v,

$$v = V_* - \frac{f_{UUU*}C_4(q_1) + 3f_{UUV*}(C_2(q_1))^2}{6(f_{UU*} + 2f_{UV*} + f_{VV*})C_2(q_1)}a_1^2 - \frac{3f_{UVV*}(C_2(q_2))^2 + f_{VVV*}C_4(q_2)}{6(f_{UU*} + 2f_{UV*} + f_{VV*})C_2(q_2)}a_2^2 + O(a_1^3) + O(a_1^2a_2) + O(a_1a_2^2) + O(a_2^3) \tag{62}$$

Using the coefficients in Eqs. (49) and (50) gives the equilibrium values of s_2 and s_3 as

$$s_2 = f_{U*} - (f_{UU*} + f_{UV*})\left[\frac{f_{UUU*}C_4(q_1) + 3f_{UUV*}(C_2(q_1))^2}{6(f_{UU*} + 2f_{UV*} + f_{VV*})C_2(q_1)}a_1^2 + \frac{3f_{UVV*}(C_2(q_2))^2 + f_{VVV*}C_4(q_2)}{6(f_{UU*} + 2f_{UV*} + f_{VV*})C_2(q_2)}a_2^2\right] + \frac{1}{6}f_{UUU*}a_1^2\frac{C_4(q_1)}{C_2(q_1)} + \frac{1}{2}f_{UVV*}a_2^2C_2(q_2) + O(a_1^3) + O(a_1^2a_2) + O(a_1a_2^2) + O(a_2^3) + O(a_1^{-1}a_2^4) \tag{63}$$

$$s_3 = f_{V*} - (f_{UV*} + f_{VV*})\left[\frac{f_{UUU*}C_4(q_1) + 3f_{UUV*}(C_2(q_1))^2}{6(f_{UU*} + 2f_{UV*} + f_{VV*})C_2(q_1)}a_1^2 + \frac{3f_{UVV*}(C_2(q_2))^2 + f_{VVV*}C_4(q_2)}{6(f_{UU*} + 2f_{UV*} + f_{VV*})C_2(q_2)}a_2^2\right] + \frac{1}{2}f_{UUV*}a_1^2C_2(q_1) + \frac{1}{6}f_{VVV*}a_2^2\frac{C_4(q_2)}{C_2(q_2)} + O(a_1^4a_2^{-1}) + O(a_1^3) + O(a_1^2a_2) + O(a_1a_2^2) + O(a_2^3) \tag{64}$$

Using Eq. (53), the equilibrium value of s_1 is

$$s_1 = f + \frac{1}{2}[f_{UU*}a_1^2C_2(q_1) + f_{VV*}a_2^2C_2(q2)] + O(a_1^3) + O(a_1^2a_2) + O(a_1a_2^2) + O(a_2^3) \tag{65}$$

And so, the average system has an equilibrium point at

$$v = V_* - \frac{f_{UUU*}C_4(q_1) + 3f_{UUV*}(C_2(q_1))^2}{6(f_{UU*} + 2f_{UV*} + f_{VV*})C_2(q_1)}a_1^2 - \frac{3f_{UVV*}(C_2(q_2))^2 + f_{VVV*}C_4(q_2)}{6(f_{UU*} + 2f_{UV*} + f_{VV*})C_2(q_2)}a_2^2 + O(a_1^3) + O(a_1^2a_2) + O(a_1a_2^2) + O(a_2^3) \tag{66a}$$

$$s_1 = f_* + \frac{1}{2}[f_{UU*}a_1^2C_2(q_1) + f_{VV*}a_2^2C_2(q2)] + O(a_1^3) + O(a_1^2a_2) + O(a_1a_2^2) + O(a_2^3) \tag{66b}$$

$$s_2 = f_{U*} - (f_{UU*} + f_{UV*})\left[\frac{f_{UUU*}C_4(q_1) + 3f_{UUV*}(C_2(q_1))^2}{6(f_{UU*} + 2f_{UV*} + f_{VV*})C_2(q_1)}a_1^2 + \frac{3f_{UVV*}(C_2(q_2))^2 + f_{VVV*}C_4(q_2)}{6(f_{UU*} + 2f_{UV*} + f_{VV*})C_2(q_2)}a_2^2\right] + \frac{1}{6}f_{UUU*}a_1^2\frac{C_4(q_1)}{C_2(q_1)} + \frac{1}{2}f_{UVV*}a_2^2C_2(q_2) + O(a_1^3) + O(a_1^2a_2) + O(a_1a_2^2) + O(a_2^3) + O(a_1^{-1}a_2^4) \tag{66c}$$

$$s_3 = f_{V*} - (f_{UV*} + f_{VV*})\left[\frac{f_{UUU*}C_4(q_1) + 3f_{UUV*}(C_2(q_1))^2}{6(f_{UU*} + 2f_{UV*} + f_{VV*})C_2(q_1)}a_1^2 + \frac{3f_{UVV*}(C_2(q_2))^2 + f_{VVV*}C_4(q_2)}{6(f_{UU*} + 2f_{UV*} + f_{VV*})C_2(q_2)}a_2^2\right] + \frac{1}{2}f_{UUV*}a_1^2C_2(q_1) + \frac{1}{6}f_{VVV*}a_2^2\frac{C_4(q_2)}{C_2(q_2)} + O(a_1^4a_2^{-1}) + O(a_1^3) + O(a_1^2a_2) + O(a_1a_2^2) + O(a_2^3) \tag{66d}$$

$$V_{\text{cmd}} = V_* - \frac{f_{UUU*}C_4(q_1) + 3f_{UUV*}(C_2(q_1))^2}{6(f_{UU*} + 2f_{UV*} + f_{VV*})C_2(q_1)}a_1^2 - \frac{3f_{UVV*}(C_2(q_2))^2 + f_{VVV*}C_4(q_2)}{6(f_{UU*} + 2f_{UV*} + f_{VV*})C_2(q_2)}a_2^2 + O(a_1^3) + O(a_1^2a_2) + O(a_1a_2^2) + O(a_2^3) \tag{66e}$$

To aid understanding, a lower-order approximation of the equilibrium point is given in the next equations.

$$v = V_* + O(a_1^2) + O(a_1a_2) + O(a_2^2) \tag{67a}$$

$$s_1 = f_* + O(a_1^2) + O(a_1a_2) + O(a_2^2) \tag{67b}$$

$$s_2 = f_{U*} + O(a_1^2) + O(a_1a_2) + O(a_2^2) + O(a_1^{-1}a_2^3) \tag{67c}$$

$$s_3 = f_{V*} + O(a_1^3a_2^{-1}) + O(a_1^2) + O(a_1a_2) + O(a_2^2) \tag{67d}$$

$$V_{\text{cmd}} = V_* + O(a_1^2) + O(a_1a_2) + O(a_2^2) \tag{67e}$$

Next, the stability of the equilibrium point is tested. The Jacobian of the average system in terms of the variables v, s_1, s_2, s_3, and V_{cmd}, evaluated at the equilibrium point $(v_{\text{eq}}, v_{\text{eq}})$, is

$$J = \begin{pmatrix} -\frac{1}{\tau} & 0 & 0 & 0 & \frac{1}{\tau} \\ J_{2,1} & -k_1 & 0 & 0 & 0 \\ J_{3,1} & 0 & -k_2a_1^2C_2(q_1) + \sigma_2k_{\text{ES}} & \sigma_2k_{\text{ES}} & 0 \\ J_{4,1} & 0 & \sigma_3k_{\text{ES}} & -k_3a_2^2C_2(q_2) + \sigma_3k_{\text{ES}} & 0 \\ 0 & 0 & k_{\text{ES}} & k_{\text{ES}} & 0 \end{pmatrix} \tag{68}$$

The expressions for the remaining elements are

$$J_{2,1} = k_1\frac{\partial}{\partial v}\left[\int_{-\infty}^{\infty}\int_{-\infty}^{\infty} f\mu(\mathrm{d}\eta_1)\mu(\mathrm{d}\eta_2)\right]\Bigg|_{v=v_{\text{eq}}} \tag{69}$$

$$J_{3,1} = k_2\frac{\partial}{\partial v}\left[\int_{-\infty}^{\infty}\int_{-\infty}^{\infty} a_1 sat\eta_1 f\mu(\mathrm{d}\eta_1)\mu(\mathrm{d}\eta_2)\right]\Bigg|_{v=v_{\text{eq}}} \tag{70}$$

$$J_{4,1} = k_3\frac{\partial}{\partial v}\left[\int_{-\infty}^{\infty}\int_{-\infty}^{\infty} a_2 sat\eta_2 f\mu(\mathrm{d}\eta_1)\mu(\mathrm{d}\eta_2)\right]\Bigg|_{v=v_{\text{eq}}} \tag{71}$$

where the partial derivatives are evaluated at the equilibrium point. The characteristic polynomial is

$$\det(sI-J)=\begin{vmatrix} s+\frac{1}{\tau} & 0 & 0 & 0 & -\frac{1}{\tau} \\ -J_{2,1} & s+k_1 & 0 & 0 & 0 \\ -J_{3,1} & 0 & s+k_2a_1^2C_2(q_1)-\sigma_2k_{\mathrm{ES}} & -\sigma_2k_{\mathrm{ES}} & 0 \\ -J_{4,1} & 0 & -\sigma_3k_{\mathrm{ES}} & s+k_3a_2^2C_2(q_2)-\sigma_3k_{\mathrm{ES}} & 0 \\ 0 & 0 & -k_{\mathrm{ES}} & -k_{\mathrm{ES}} & s \end{vmatrix}$$

$$\begin{aligned} &= (s+k_1)\Bigg\{s^4+\left[k_2a_1^2C_2(q_1)+k_3a_2^2C_2(q_2)-k_{ES}(\sigma_3+\sigma_2)+\frac{1}{\tau}\right]s^3 \\ &+[k_2k_3a_1^2a_2^2C_2(q_1)C_2(q_2)-k_{\mathrm{ES}}(\sigma_2k_3a_2^2C_2(q_2)+\sigma_3k_2a_1^2C_2(q_1))+\frac{1}{\tau}(k_2a_1^2C_2(q_1) \\ &+k_3a_2^2C_2(q_2)-k_{\mathrm{ES}}(\sigma_3+\sigma_2))]s^2+\left[\frac{1}{\tau}(k_2k_3a_1^2a_2^2C_2(q_1)C_2(q_2)-k_{\mathrm{ES}}(\sigma_2k_3a_2^2C_2(q_2) \\ &+\sigma_3k_2a_1^2C_2(q_1)+J_{3,1}+J_{4,1}))\right]s+\left[-\frac{1}{\tau}k_{ES}(J_{4,1}k_2a_1^2C_2(q_1)+J_{3,1}k_3a_2^2C_2(q_2))\right]\Bigg\} \end{aligned} \tag{72}$$

The $\dot{s}_1$ dynamics decouple from the rest of the system, leaving a fourth-order polynomial. (The $\dot{s}_1$ dynamics are stable for any positive k_1.) The coefficients of the remaining fourth-order polynomial must all be positive for the system to be stable. In addition, using the Routh–Hurwitz criteria to examine a polynomial of the form $s^4+bs^3+cs^2+ds+e$, it can be shown that, if the inequality $bcd>b^2e+d^2$ holds, then the system is stable.

The s^3 and s^2 coefficients are positive if the gains k_2, k_3, and k_{ES} are chosen positive and the parameters σ_2 and σ_3 are chosen negative, but the remaining stability conditions depend on $J_{3,1}$ and $J_{4,1}$. To keep the analysis applicable to a general map, approximations are sought that are valid for small turbulence intensities.

Now, the lift to drag ratio f is a function of U and V, but both U and V can be written as functions of v [see Eq. (37)]. The lift to drag ratio can be approximated using a Taylor expansion around an arbitrary point (v,v),

$$\begin{aligned} f &= f_v+[f_{Uv}(U-v)+f_{Vv}(V-v)] \\ &+\frac{1}{2}[f_{UUv}(U-v)^2+2f_{UVv}(U-v)(V-v) \\ &+f_{VVv}(V-v)^2]+O((U-v)^3)+O((U-v)^2(V-v)) \\ &+O((U-v)(V-v)^2)+O((V-v)^3) \end{aligned} \tag{73}$$

Here, the notation f_v is used to refer to the value of f at the arbitrary point (v,v) as f_0 was used to refer to the value of f at the point (n_0,n_0) earlier in the paper; it does not denote a derivative with respect to v. Substituting Eq. (37) into Eq. (73) gives

$$\begin{aligned} f &= f_v+[f_{Uv}(a_1\mathrm{sat}\eta_1)+f_{Vv}(a_2\mathrm{sat}\eta_2)] \\ &+\frac{1}{2}[f_{UUv}(a_1\mathrm{sat}\eta_1)^2+2f_{UVv}(a_1\mathrm{sat}\eta_1)(a_2\mathrm{sat}\eta_2) \\ &+f_{VVv}(a_2\mathrm{sat}\eta_2)^2]+O((a_1\mathrm{sat}\eta_1)^3)+O((a_1\mathrm{sat}\eta_1)^2a_2\mathrm{sat}\eta_2) \\ &+O(a_1\mathrm{sat}\eta_1(a_2\mathrm{sat}\eta_2)^2)+O((a_2\mathrm{sat}\eta_2)^3) \end{aligned} \tag{74}$$

Using this expression for f, the integrals in Eqs. (70) and (71) can be evaluated. After simplification, they reduce to

$$\begin{aligned} \int_{-\infty}^{\infty}\int_{-\infty}^{\infty}a_1\mathrm{sat}\eta_1 f\mu(\mathrm{d}\eta_1)\mu(\mathrm{d}\eta_2) &= f_{Uv}a_1^2C_2(q_1) \\ &+O(a_1^4)+O(a_1^3a_2)+O(a_1^2a_2^2)+O(a_1a_2^3) \end{aligned} \tag{75}$$

$$\begin{aligned} \int_{-\infty}^{\infty}\int_{-\infty}^{\infty}a_2\mathrm{sat}\eta_2 f\mu(\mathrm{d}\eta_1)\mu(\mathrm{d}\eta_2) &= f_{Vv}a_2^2C_2(q_2) \\ &+O(a_1^3a_2)+O(a_1^2a_2^2)+O(a_1a_2^3)+O(a_2^4) \end{aligned} \tag{76}$$

Now, because U and V both vary directly with v, the partial derivative with respect to v can be expressed as the sum of the partial derivatives with respect to U and V,

$$\frac{\partial}{\partial v}=\frac{\partial}{\partial U}\frac{\partial U}{\partial v}+\frac{\partial}{\partial V}\frac{\partial V}{\partial v}=\frac{\partial}{\partial U}+\frac{\partial}{\partial V} \tag{77}$$

Taking these partial derivatives of the integrals (75) and (76) and evaluating at the equilibrium point $(v_{\mathrm{eq}},v_{\mathrm{eq}})$ gives

$$\begin{aligned} J_{3,1} &= k_2\frac{\partial}{\partial v}\left[\int_{-\infty}^{\infty}\int_{-\infty}^{\infty}a_1\mathrm{sat}\eta_1 f\mu(\mathrm{d}\eta_1)\mu(\mathrm{d}\eta_2)\right]\Bigg|_{v=v_{\mathrm{eq}}} \\ &= k_2\left(\frac{\partial}{\partial U}[f_{Uv}]+\frac{\partial}{\partial V}[f_{Uv}]\right)\Bigg|_{v=v_{\mathrm{eq}}}a_1^2C_2(q_1)+O(a_1^4) \\ &+O(a_1^3a_2)+O(a_1^2a_2^2)+O(a_1a_2^3) \\ &= k_2(f_{UU\mathrm{eq}}+f_{UV\mathrm{eq}})a_1^2C_2(q_1)+O(a_1^4) \\ &+O(a_1^3a_2)+O(a_1^2a_2^2)+O(a_1a_2^3) \end{aligned} \tag{78a}$$

and similarly,

$$\begin{aligned} J_{4,1} &= k_3(f_{UV\mathrm{eq}}+f_{VV\mathrm{eq}})a_2^2C_2(q_2)+O(a_1^3a_2)+O(a_1^2a_2^2) \\ &+O(a_1a_2^3)+O(a_2^4) \end{aligned} \tag{78b}$$

Because these are already small a_1 and a_2 approximations, note that the preceding expressions can be equivalently stated in terms of the second partial derivatives at the maximum of the map, because for small a_1 and a_2 the equilibrium point approaches the maximum of the map. That is, because

$$v_{\mathrm{eq}}=V_*+O(a_1^2)+O(a_1a_2)+O(a_2^2) \tag{79}$$

we can say

$$f_{UU\mathrm{eq}}=f_{UU*}+O(a_1^2)+O(a_1a_2)+O(a_2^2) \tag{80}$$

and similarly with other derivatives. Then,

$$\begin{aligned} J_{3,1} &= k_2(f_{UU*}+f_{UV*})a_1^2C_2(q_1)+O(a_1^4)+O(a_1^3a_2) \\ &+O(a_1^2a_2^2)+O(a_1a_2^3) \end{aligned} \tag{81a}$$

$$\begin{aligned} J_{4,1} &= k_3(f_{UV*}+f_{VV*})a_2^2C_2(q_2)+O(a_1^3a_2)+O(a_1^2a_2^2) \\ &+O(a_1a_2^3)+O(a_2^4) \end{aligned} \tag{81b}$$

With these approximations, the characteristic polynomial can be written for small a_1 and a_2 as

$$(s+k_1)\Bigg\{s^4+\left[-k_{\mathrm{ES}}(\sigma_3+\sigma_2)+\frac{1}{\tau}+O(a_1^2)+O(a_2^2)\right]s^3 + \left[-\frac{k_{\mathrm{ES}}}{\tau}(\sigma_3+\sigma_2)+O(a_1^2)+O(a_2^2)\right]s^2 + \Bigg[-\frac{k_{\mathrm{ES}}}{\tau}(k_2(f_{UU*}+f_{UV*}+\sigma_3)a_1^2C_2(q_1) + k_3(f_{UV*}+f_{VV*}+\sigma_2)a_2^2C_2(q_2))+O(a_1^4) + O(a_1^3a_2)+O(a_1^2a_2^2)+O(a_1a_2^3)+O(a_2^4)\Bigg]s + \Bigg[-\frac{1}{\tau}k_{\mathrm{ES}}k_2k_3a_1^2a_2^2C_2(q_1)C_2(q_2)(f_{UU*}+2f_{UV*}+f_{VV*}) + O(a_1^5a_2)+O(a_1^4a_2^2)+O(a_1^3a_2^3)+O(a_1^2a_2^4)+O(a_1a_2^5)\Bigg]\Bigg\} \quad (82)$$

Now the stability criteria can be tested. Again, k_1 must be positive,

$$k_1 > 0 \quad (83a)$$

For small a_1 and a_2, the s^3 and s^2 coefficients are positive provided k_{ES} is positive and the sum$\sigma_3+\sigma_2$ is negative,

$$k_{\mathrm{ES}} > 0 \quad (83b)$$

$$(\sigma_3+\sigma_2) < 0 \quad (83c)$$

Similarly, the s^1 coefficient is positive provided that (in addition to k_{ES} being chosen positive) k_2 and k_3 are positive and σ_2 and σ_3 are chosen sufficiently negative. Specifically, if

$$k_2 > 0 \quad (83d)$$

$$k_3 > 0 \quad (83e)$$

and

$$\sigma_3 < -(f_{UU*}+f_{UV*}) \quad (83f)$$

$$\sigma_2 < -(f_{UV*}+f_{VV*}) \quad (83g)$$

Note that the s^1 coefficient cannot be made positive by choosing k_{ES} small because k_{ES} multiplies the entire coefficient (for the small a_1, a_2 approximation, at least). Finally, for small a_1 and a_2, the s^0 coefficient is positive provided that k_{ES}, k_2, and k_3 are chosen positive. [Recall from Eq. (55) that, because we assume a unique maximum point along the line $U=V$, it follows that $f_{UU*}+2f_{UV*}+f_{VV*}<0$.]

And so, in the analysis of the characteristic polynomial, the conditions under which all of the coefficients are positive have been found. For stability, it remains to be shown that (in terms of a polynomial of the form $s^4+bs^3+cs^2+ds+e$) the inequality $bcd > b^2e+d^2$ holds. The stability criterion simplifies to

$$\left[-k_{\mathrm{ES}}(\sigma_3+\sigma_2)+\frac{1}{\tau}\right]\times\left[\frac{1}{\tau}(-k_{\mathrm{ES}}(\sigma_3+\sigma_2))\right] \times\left[-\frac{k_{\mathrm{ES}}}{\tau}(k_2(f_{UU*}+f_{UV*}+\sigma_3)a_1^2C_2(q_1) + k_3(f_{UV*}+f_{VV*}+\sigma_2)a_2^2C_2(q_2))\right] > 0 + O(a_1^4)+O(a_1^3a_2)+O(a_1^2a_2^2)+O(a_1a_2^3)+O(a_2^4) \quad (84)$$

This criterion is satisfied for small a_1 and a_2 under the criteria already required to ensure the coefficients of the characteristic polynomial are positive. The equilibrium (66) of the closed-loop system (23) is stable for small a_1 and a_2 under the conditions (83).

The conditions on σ_2 and σ_3 can be simplified somewhat. Given from Eq. (55) that $f_{UU*}+2f_{UV*}+f_{VV*}<0$, the following inequalities hold:

$$\frac{1}{2}(f_{VV*}-f_{UU*}) < -(f_{UU*}+f_{UV*}) \quad (85a)$$

$$\frac{1}{2}(f_{UU*}-f_{VV*}) < -(f_{UV*}+f_{VV*}) \quad (85b)$$

If the parameters σ_2 and σ_3 are chosen according to

$$\sigma_3 < \frac{1}{2}(f_{VV*}-f_{UU*}) \quad (86a)$$

$$\sigma_2 < \frac{1}{2}(f_{UU*}-f_{VV*}) \quad (86b)$$

then Eqs. (83c), (83f), and (83g) are satisfied.

This concludes the bulk of the analysis. The average system has a stable equilibrium at the point given in Eq. (66), which is within an $O(a_1^2)+O(a_1a_2)+O(a_2^2)$ neighborhood of the optimal endurance speed. The linearized average system is stable if the turbulence intensities a_1 and a_2 are small but nonzero; the gains k_1, k_2, k_3, and k_{ES} are chosen positive; and the design parameters σ_2 and σ_3 are chosen to satisfy the criteria given in Eq. (86). Stability of the linearized average system proves the local exponential stability of the average system (34) by Corollary 4.3 in [34]. Stability of the average system proves the weak stability of the closed-loop system (23) under the stochastic perturbations η_1 and η_2, by the stochastic averaging results in [8]. This result is expressed in Theorem 1.

Simulations

Simple Simulation

Before proceeding to the high-fidelity simulations, the results of a simpler simulation are presented. This simulation follows Eq. (23) closely. The parameters of the simulation are listed in Table 1. They are chosen roughly to represent a U-2 flying at maximum takeoff weight at 36,000 ft. The turbulence parameters are chosen to model an isotropic turbulence with a root mean square intensity of 3 ft/s and a characteristic length of 1750 ft. To align with the assumptions of the

Table 1 Simulation parameters

Parameter	Value	Units
a_1	100	ft/s
a_2	100	ft/s
ϵ_1	4.00	s
ϵ_2	4.00	s
q_1	0.225	$s^{1/2}$
q_2	0.0424	$s^{1/2}$
mg	40000	lb · f
C_{D0}	0.0106	— —
A	10.6	— —
e	1	— —
S	1000	ft^2
ρ	0.00070449	$slug/ft^3$
a	968.08	ft/s
τ	5	s
k_1	0.200	1/s
k_2	1.98×10^{-4}	s/ft^2
k_3	0.00556	s/ft^2
k_{ES}	22.9	ft^2/s^3
σ_2	-6.53×10^{-4}	s^2/ft^2
σ_3	0.00	s^2/ft^2

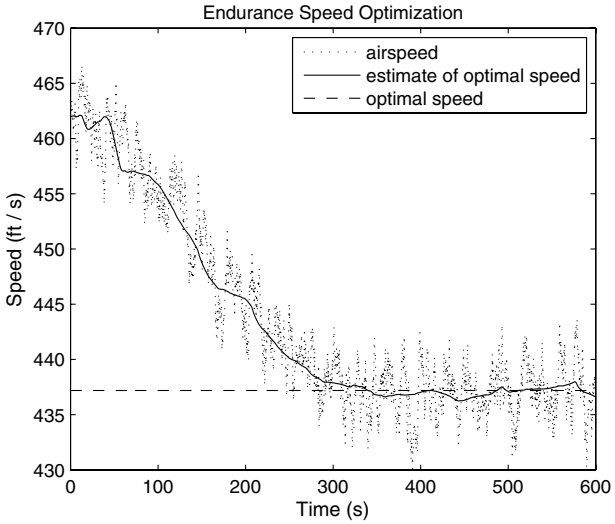

Fig. 2 Results of a simulation closely following Eq. (23).

analysis, the turbulence is bounded to less than 100 ft/s. The lift to drag ratio is modeled assuming a quadratic drag polar and using the Prandtl–Glauert rule. Written as a function of the equivalent steady-state airspeed and airspeed, the lift to drag ratio is

$$f(U,V)=\frac{\frac{2mg}{U^2\rho S}}{C_{D0}+\frac{1}{\pi Ae}\left(\frac{2mg}{U^2\rho S}\right)^2\left(1-\left(\frac{V}{a}\right)^2\right)} \tag{87}$$

The constants in this formula are given Table 1. The controller gains and design parameters are also listed. The results of this simple simulation are shown in Fig. 2.

The simulation represents a situation in which the drag coefficient is 21 drag counts higher than predicted during the design. The starting airspeed in this simulation is 462 ft/s, which is the optimal endurance speed if the zero-lift drag coefficient C_{D0} is 0.0085 instead of 0.0106. At this airspeed, the aircraft has a lift to drag ratio of 31.00. Flying at the optimal airspeed (about 437 ft/s) the lift to drag ratio is 31.21. This represents a decrease in the drag of 0.67% and a corresponding improvement in the endurance.

High-Fidelity Simulation Description

The software used for the following simulations is a six-degree-of-freedom simulation routine developed by local industry. Because of the proprietary nature of the simulation, the simulation cannot be described in detail, but the simulation is highly realistic and has been validated by flight test data. To prevent disclosure of proprietary aircraft performance data, the numbers have been removed from all the axes of the figures showing high-fidelity simulation results.

Experiment Design

Two experiments are performed using the high-fidelity simulation software. The first is designed to test the extremum-seeking algorithm. The simulation begins with the aircraft flying straight and level at its nominal loiter speed. The aircraft then encounters turbulence, and the extremum-seeking algorithm is activated; the aircraft adjusts its airspeed to the estimate of the optimal airspeed found by the algorithm. The turbulence encounter then ends, and the extremum-seeking control law is disengaged. From this point on, the airspeed command is set to maintain the same coefficient of lift as found by the extremum-seeking algorithm. The simulation is then allowed to run for a short time to allow the transients to settle. For comparison, the simulation is repeated without activating the extremum-seeking algorithm. The steady fuel flow rate achieved by the extremum-seeking algorithm is then compared to the steady fuel flow rate at the nominal loiter speed. A lower fuel flow rate corresponds to a higher endurance.

The second experiment is designed to test the effectiveness of holding a constant coefficient of lift after the turbulence encounter ends. The experiment is similar to the first, with the following changes. The experiment runs for a much longer period of time, during which significant changes in aircraft weight occur due to fuel being burned. The experiment is also run using settings of higher realism in the simulation software, which make for a good experiment but poor graphs, and as such are not used in the first experiment. Like the first experiment, the second experiment consists of two simulations that are identical, except that, in one, extremum seeking is active and in the other the aircraft remains at the nominal loiter speed. The aircraft weight decreases in both simulations as fuel is burned. The difference between the aircraft weights indicates the net fuel savings from extremum seeking.

Note that, because this is a computer simulation, the nominal loiter speed is expected to be at or very near the optimal endurance speed. The primary benefit of extremum seeking is that it is able to adapt to differences from the aerodynamic model that may exist in real flight. These simulations do not introduce any such differences, and so the level of endurance achieved by extremum seeking is expected to be only as good as that achieved by the nominal loiter speed. The simulations test the ability of extremum seeking to achieve a level of endurance on par with that achieved by the nominal loiter speed in simulation, which provides a measure of confidence in the ability of the algorithm to find the true optimal endurance speed in real flight.

High-Fidelity Simulation Results

The results of the first experiment are shown in Figs. 3–5. In these figures, results using the extremum-seeking algorithm are shown in black; the results not using extremum seeking are shown in the background in gray. The small region boxed in Fig. 4 is shown enlarged in Fig. 5.

The results of the second experiment are shown in Fig. 6. The aircraft weight over the course of the simulations is plotted against the left axis, again in black for the results using extremum seeking and gray for the results not using extremum seeking. Because the curves overlap almost identically, the difference between the two curves is plotted in the same figure against the right axis, as a dashed line, on a much larger scale. Note that the difference is initially zero and becomes positive, indicating that the weight of the aircraft using

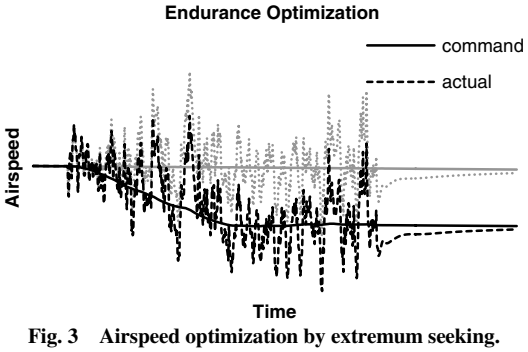

Fig. 3 Airspeed optimization by extremum seeking.

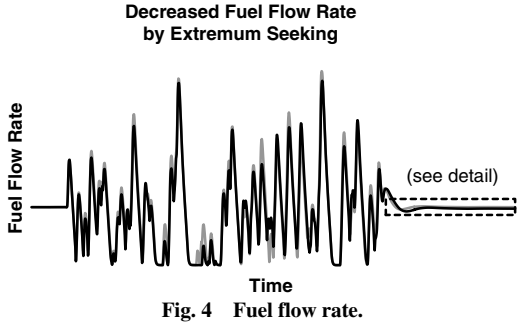

Fig. 4 Fuel flow rate.

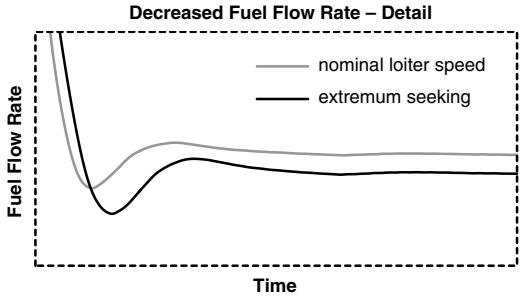

Fig. 5 Fuel flow rate detail plot.

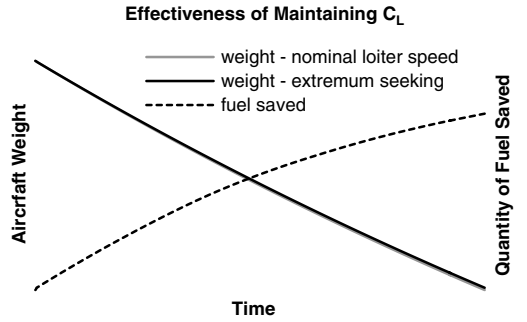

Fig. 6 Net fuel savings over a long flight achieved by flying a constant C_L after exiting turbulence.

extremum seeking is greater than that of the aircraft at the nominal loiter speed.

Discussion

The simulation results show that the extremum-seeking algorithm matches the fuel economy of the flight at the nominal loiter speed in simulation, without knowledge of the performance characteristics of the aircraft (see Fig. 4). The algorithm slightly exceeds the performance achieved at the nominal loiter speed; the difference is small but noticeable (Fig. 5). In simulations based on wind-tunnel data, the nominal loiter speed should be close to the optimal endurance speed; the fact that the simulations show convergence to near the nominal loiter speed (with actually even slightly better performance) gives some confidence that the optimal speed may be found regardless of the aerodynamic characteristics of the aircraft. The benefit of the algorithm is not primarily in the slight performance improvements shown in these figures. Rather, the benefit is in the potentially more significant improvements that might be achieved in actual flight where the aerodynamic characteristics of the aircraft may differ from the wind-tunnel data. Such differences may appear over time due to accumulated minor damage to the plane or due to environmental conditions such as structural icing. In such situations, the endurance benefits from extremum seeking may become significant.

As shown in Fig. 6, the performance obtained by extremum seeking is maintained after exiting turbulence by adjusting the airspeed to fly a constant coefficient of the lift. The difference between the aircraft weight in the simulation using extremum seeking and the aircraft weight in the simulation at the nominal loiter speed, shown as the dashed line in Fig. 6, consistently increases throughout the simulation. This indicates that the aircraft using extremum seeking continues to burn fuel at a slower rate than the aircraft at the nominal loiter speed throughout the flight, even though extremum seeking is only active for a short period of time at the beginning of the flight.

The simulation results also confirm the stability analysis performed in the preceding sections. This may lend some credence to the modeling assumptions used in the analysis. A limitation of the result in Theorem 1 is that it speaks to the limiting case as the turbulence timescales ϵ_1 and ϵ_2 approach zero. Stated another way, the theorem describes the behavior of the system when all timescales are slow compared to the turbulence timescales. As such, the theorem does not make any claim regarding the behavior of the system on timescales comparable to the turbulence. Because the high-fidelity simulation results are presented without units, the simple simulation results shown in Fig. 2 are presented to speak to the rate of convergence of the algorithm. (Again, to avoid inadvertently revealing any aircraft performance data, the parameters used in the simple simulations are not the same as those used in the high-fidelity simulations.)

Another limitation of the result in Theorem 1 is that it applies only when the turbulence is small but nonzero. The controller cannot function in calm air, and it is also possible that the controller could become unstable in unexpectedly heavy turbulence. Although the intensity of the turbulence can never be controlled, the design parameters can be adjusted to ensure stability in a worst-case turbulence encounter.

One area that remains to be addressed is operation in turning flight. The analysis and simulations above all assume straight and level flight, but loitering is commonly performed in a holding pattern, which involves portions of turning flight and portions of straight flight. The algorithm may require a modification to be applicable to turning flight.

Conclusions

The extremum-seeking algorithm stabilizes the aircraft to near the optimal endurance speed, accounting for both angle of attack and compressibility effects, using the excitation provided by atmospheric turbulence. Simulation results using a high-fidelity aircraft simulation routine show that the algorithm achieves a level of endurance slightly greater than that at the nominal loiter speed of the aircraft. This provides confidence that the optimal airspeed may be achieved in real flight where the aerodynamic characteristics of the aircraft are not known. The results validate the performance of the new form of gradient estimator used in the extremum-seeking algorithm. After a turbulence encounter has ended, flying a constant coefficient of the lift is an adequate means of maintaining the optimal airspeed as the aircraft weight decreases.

Acknowledgments

This work was supported in part by the San Diego chapter of the Achievement Rewards for College Scientists (ARCS) Foundation. The authors would also like to thank the representatives of local industry who made possible the high-fidelity simulations.

References

[1] Krieger, J. P., and Krstic, M., "Extremum Seeking Based on Atmospheric Turbulence for Aircraft Endurance," *Journal of Guidance, Control, and Dynamics*, Vol. 34, No. 6, 2011, pp. 1876–1885. doi:10.2514/1.53825

[2] Ariyur, K. B., and Krstic, M., "SISO Scheme and Linear Analysis," *Real-Time Optimization by Extremum-Seeking Control*, Wiley, Hoboken, NJ, 2003, pp. 3–20.

[3] Wang, H.-H., and Krstic, M., "Extremum Seeking for Limit Cycle Minimization," *IEEE Transactions on Automatic Control*, Vol. 45, No. 12, Dec. 2000, pp. 2432–2436. doi:10.1109/9.895589

[4] Choi, J.-Y., Krstic, M., Ariyur, K. B., and Lee, J. S., "Extremum Seeking Control for Discrete-Time Systems," *IEEE Transactions on Automatic Control*, Vol. 47, No. 2, Feb. 2002, pp. 318–323. doi:10.1109/9.983370

[5] Rotea, M. A., "Analysis of Multivariable Extremum Seeking Algorithms," *Proceedings of the American Control Conference*, IEEE Publications, Piscataway, NJ, 2000, pp. 433–437. doi:10.1109/ACC.2000.878937

[6] Adetola, V., and Guay, M., "Parameter Convergence in Adaptive Extremum-Seeking Control," *Automatica*, Vol. 43, No. 1, 2007, pp. 105–110. doi:10.1016/j.automatica.2006.07.021

[7] Tan, Y., Nesic, D., and Mareels, I., "On the Choice of Dither in Extremum Seeking Systems: A Case Study," *Automatica*, Vol. 44, No. 5, 2008, pp. 1446–1450. doi:10.1016/j.automatica.2007.10.016

[8] Liu, S.-J., and Krstic, M., "Stochastic Averaging in Continuous Time and its Applications to Extremum Seeking," *IEEE Transactions on*

Automatic Control, Vol. 55, No. 10, Oct. 2010, pp. 2235–2250. doi:10.1109/TAC.2010.2043290

[9] Manzie, C., and Krstic, M., "Extremum Seeking with Stochastic Perturbations," *IEEE Transactions on Automatic Control*, Vol. 54, No. 3, 2009, pp. 580–585. doi:10.1109/TAC.2008.2008320

[10] Carnevale, D., Astolfi, A., Centioli, C., Podda, S., Vitale, V., and Zaccarian, L., "A New Extremum Seeking Technique and its Application to Maximize RF Heating on FTU," *Fusion Engineering and Design*, Vol. 84, Nos. 2–6, 2009, pp. 554–558. doi:10.1016/j.fusengdes.2008.12.032

[11] Wang, H.-H., Yeung, S., and Krstic, M., "Experimental Application of Extremum Seeking on an Axial-Flow Compressor," *IEEE Transactions on Control Systems Technology*, Vol. 8, No. 2, Mar. 2000, pp. 300–309. doi:10.1109/87.826801

[12] Moeck, J. P., Bothien, M. R., Paschereit, C. O., Gelbert, G., and King, R., "Two-Parameter Extremum Seeking for Control of Thermoacoustic Instabilities and Characterization of Linear Growth," AIAA Paper 2007-1416, Jan. 2007.

[13] Moase, W. H., Manzie, C., and Brear, M. J., "Newton-Like Extremum-Seeking for the Control of Thermoacoustic Instability," *IEEE Transactions on Automatic Control*, Vol. 55, No. 9, 2010, pp. 2094–2105. doi:10.1109/TAC.2010.2042981

[14] Banaszuk, A., Ariyur, K. B., Krstic, M., and Jacobson, C. A., "An Adaptive Algorithm for Control of Combustion Instability," *Automatica*, Vol. 40, No. 11, 2004, pp. 1965–1972. doi:10.1016/j.automatica.2004.06.008

[15] Becker, R., King, R., Petz, R., and Nitsche, W., "Adaptive Closed-Loop Separation Control on a High-Lift Configuration Using Extremum Seeking," *AIAA Journal*, Vol. 45, No. 6, 2007, pp. 1382–1392. doi:10.2514/1.24941

[16] Kim, K., Kasnakoglu, C., Serrani, A., and Samimy, M., "Extremum-Seeking Control of Subsonic Cavity Flow," *AIAA Journal*, Vol. 47, No. 1, 2009, pp. 195–205. doi:10.2514/1.38180

[17] Creaby, J., Li, Y., and Seem, J. E., "Maximizing Wind Turbine Energy Capture using Multivariable Extremum Seeking Control," *Wind Engineering*, Vol. 33, No. 4, 2009, pp. 361–387. doi:10.1260/030952409789685753

[18] Binetti, P., Ariyur, K. B., Krstic, M., and Bernelli, F., "Formation Flight Optimization Using Extremum Seeking Feedback," *Journal of Guidance, Control, and Dynamics*, Vol. 26, No. 1, 2003, pp. 132–142. doi:10.2514/2.5024

[19] Stankovic, M. S., and Stipanovic, D. M., "Extremum Seeking Under Stochastic Noise and Applications to Mobile Sensors," *Automatica*, Vol. 46, No. 8, 2010, pp. 1243–1251. doi:10.1016/j.automatica.2010.05.005

[20] Stankovic, M., Johansson, K., and Stipanovic, D., "Distributed Seeking of Nash Equilibria with Applications to Mobile Sensor Networks," *IEEE Transactions on Automatic Control*, Vol. 57, No. 4, 2012, pp. 904–919. doi:10.1109/TAC.2011.2174678

[21] Tanelli, M., Astolfi, A., and Savaresi, S. M., "Non-Local Extremum Seeking Control for Active Braking Control Systems," *Proceedings of the 2006 IEEE International Conference on Control Applications*, IEEE Publications, Piscataway, NJ, 2006, pp. 891–896. doi:10.1109/CACSD-CCA-ISIC.2006.4776763

[22] Schuster, E., Xu, C., Torres, N., Morinaga, E., Allen, C., and Krstic, M., "Beam Matching Adaptive Control via Extremum Seeking," *Nuclear Instruments and Methods*, Vol. 581, No. 3, 2007, pp. 799–815. doi:10.1016/j.nima.2007.07.154

[23] Bastin, G., Nešić, D., Tan, Y., and Mareels, I., "On Extremum Seeking in Bioprocesses with Multivalued Cost Functions," *Biotechnology Progress*, Vol. 25, No. 3, 2009, pp. 683–689. doi:10.1002/btpr.v25:3

[24] Ou, Y., Xu, C., Schuster, E., Luce, T. C., Ferron, J. R., Walker, M. L., and Humphreys, D. A., "Design and Simulation of Extremum-Seeking Open-Loop Optimal Control of Current Profile in the DIII-D Tokamak," *Plasma Physics and Controlled Fusion*, Vol. 50, No. 11, 2008, p. 115001. doi:10.1088/0741-3335/50/11/115001

[25] Zhang, C., Arnold, D., Ghods, N., Siranosian, A., and Krstic, M., "Source Seeking with Non-Nolonomic Unicycle Without Position Measurement and with Tuning of Forward Velocity," *Systems and Control Letters*, Vol. 56, No. 3, 2007, pp. 245–252. doi:10.1016/j.sysconle.2006.10.014

[26] Cochran, J., and Krstic, M., "Nonholonomic Source Seeking with Tuning of Angular Velocity," *IEEE Transactions on Automatic Control*, Vol. 54, No. 4, 2009, pp. 717–731. doi:10.1109/TAC.2009.2014927

[27] Liu, S.-J., and Krstic, M., "Stochastic Source Seeking for Nonholonomic Unicycle," *Automatica*, Vol. 46, No. 9, 2010, pp. 1443–1453. doi:10.1016/j.automatica.2010.05.025

[28] Zhang, X., Dawson, D., Dixon, W., and Xian, B., "Extremum-Seeking Nonlinear Controllers for a Human Exercise Machine," *IEEE/ASME Transactions on Mechatronics*, Vol. 11, No. 2, 2006, pp. 233–240. doi:10.1109/TMECH.2006.871896

[29] Li, Y., Rotea, M., Chiu, G.-C., Mongeau, L., and Paek, I.-S., "Extremum Seeking Control of a Tunable Thermoacoustic Cooler," *IEEE Transactions on Control Systems Technology*, Vol. 13, No. 4, 2005, pp. 527–536. doi:10.1109/TCST.2005.847334

[30] Killingsworth, N. J., and Krstic, M., "PID Tuning Using Extremum Seeking: Online, Model-Free Performance Optimization," *IEEE Control Systems*, Vol. 26, No. 1, 2006, pp. 70–79. doi:10.1109/MCS.2006.1580155

[31] "Flying Qualities of Piloted Airplanes," U.S. Military Specification MIL-F-8785C, 1980.

[32] Phillips, W. F., "Aircraft Performance," *Mechanics of Flight*, Wiley, Hoboken, NJ, 2004, pp. 221–338.

[33] Moran, J., "Compressible Potential Flow past Airfoils," *An Introduction to Theoretical and Computational Aerodynamics*, Dover, Mineola, NY, 2003, pp. 381–423.

[34] Khalil, H. K., *Nonlinear Systems*, 3rd ed., Prentice–Hall, Upper Saddle River, NJ, 2002, p. 166.